

Effects of agricultural terraces on landslide occurrence: insights from a tropical mountainous region (Rwanda, Africa)

Pascal Sibomana^{a,b,*}, Matthias Vanmaercke^c, Arthur Depicker^c, Bernard Tychon^a, Aurélie Hubert^a, Olivier Dewitte^d

^a UR SPHERES, University of Liège, Liège, Belgium

^b Department of Civil Engineering, INES-Ruhengeri, Musanze, Rwanda

^c Department of Earth and Environmental Sciences, KU Leuven, Belgium

^d Department of Earth Sciences, Royal Museum for Central Africa, Tervuren, Belgium

ABSTRACT

Agricultural terraces are a commonly applied soil and water conservation strategy on steep and intensely cultivated hillslopes. Yet agricultural terraces can lead to an increased incidence of landslides. Nevertheless, their effects on hillslope stability remain poorly studied, especially in the tropical Global South, where terraces are increasingly implemented. Here we investigate to what extent the presence of such terraces may increase the incidence of landslides in the densely-populated northwestern Rwanda. For this, we mapped three important landslide events that were triggered by distinct and intense rainfall events in the region and analyzed the relation of these landslides to the presence of terraces and other controlling factors. Based on an inventory of >4,600 mostly shallow landslides in these three events, we show that landslides are about three times more likely to occur on terraced hillslopes as compared to non-terraced hillslopes. However, our results also demonstrate important variability between the events. While the effect was most pronounced for the largest 2020-event, the other two events, 2016 and 2018, showed a less clear or even negative impact of terracing on landslide occurrence. Furthermore, we observed this effect mainly on moderately to highly susceptible hillslopes and less so in areas with a very high landslide susceptibility. Landslides on terraces also tend to be slightly smaller than their counterparts in non-terraced areas. These findings have important implications for both landslide susceptibility assessment and land management.

* Corresponding authors : Pascal.Sibomana@student.uliege.be (P. Sibomana), matthias.vanmaercke@kuleuven.be (M. Vanmaercke), olivier.dewitte@africamuseum.be (O. Dewitte).

30 *Keywords:* Mass movement; agricultural terraces; landslide inventory; tropical environment;
31 rainfall, susceptibility modelling

32

33 **1. Introduction**

34 Landslides are common and often impactful hillslope hazards caused by a range of natural and/or
35 human-induced controlling factors (Sidle and Bogaard, 2016). For example, hillslopes of similar
36 morphologies but underlain by different lithologies can lead to landslides of different types, sizes
37 and frequencies (Clarke and Burbank, 2010; Mugaruka Bibentyo et al., 2024). Landsliding is also
38 often influenced by vegetation characteristics (Gabet and Dunne, 2002; Zhou et al., 2002; Glade,
39 2003; Rickli and Graf, 2009; Wolter et al., 2010; Maki Mateso et al., 2023) as well as by land
40 management practices that modify hillslope morphology (Schuster and Highland, 2001; Glade,
41 2003; Crosier and Glade, 2005; Petley et al., 2007; Glade et al., 2012; Chen and Huang, 2013).
42 One of the most widely applied and significant anthropogenic hillslope modifications is
43 agricultural terraces (Brown et al., 2021). Agricultural terraces are often implemented as a soil and
44 water conservation measure (Gardner and Gerrard, 2003; Londoño 2008; Dotterweich, 2013; Deng
45 et al., 2021; Rutebuka et al., 2021) or to increase land productivity (Posthumus, 2005; Rutebuka
46 et al., 2021). More specifically, agricultural terracing reshapes natural slopes in a series of steep
47 walls (or risers) and flat surfaces (treads), often consisting of unconsolidated material (Brown et
48 al., 2021; Dorren and Rey, 2004; FAO, 2000). This not only leads to local increases in soil/regolith
49 but also reduces hillslope runoff and increases water infiltration, resulting in overall higher
50 moisture contents (Crosta et al., 2003; Sidle et al., 2006; Arnáez et al., 2015; Al Qudah et al.,
51 2016).

52 Yet, these effects may also come with downsides. Studies indicate that agricultural terraces can
53 lead to slope failure mechanisms of different types (Crosta et al., 2003; Turkelboom et al., 2008;
54 Cevasco et al., 2013; Agnoletti et al., 2019), resulting in potentially increased landslide
55 susceptibility, frequencies and/or sizes (Crosta et al., 2003; Chen et al., 2023). Nevertheless, the
56 effects of agricultural terraces on landsliding remain poorly studied, especially in the tropical
57 Global South (Sidle et al., 2006; Lewis et al., 2015; Wei et al., 2016). This corresponds to an
58 overall lack of research on landslide occurrence, susceptibility, hazard and risks in these regions,
59 especially in sub-Saharan Africa (Gariano and Guzzetti, 2016; Maes et al., 2017; Broeckx et al.,

60 2018; Reichenbach et al., 2018; Dewitte et al., 2022). Tropical mountainous regions of the Global
61 South are among the most critical regions in terms of landslide risks. The naturally high landslide
62 susceptibility of these regions, combined with their high population density, land use pressure, and
63 associated land use changes such as deforestation and urbanization, often increase the exposure of
64 an already vulnerable population to landslide hazards (Seto et al., 2012; Lewis et al., 2015;
65 Depicker et al., 2021b; Dille et al., 2022; Ozturk et al., 2022). It is also in these tropical, densely-
66 populated regions that agricultural terraces have often been implemented at massive scales
67 (Williams, 1990; Posthumus, 2005; Amsalu and de Graaff, 2006; de Graaff et al., 2008). From an
68 erosion-control and agricultural perspective, the construction of such terraces may be a valid
69 choice (e.g., Brown et al., 2021; Deng et al., 2021; Uwacu et al., 2021). Nonetheless, as terracing
70 may potentially also lead to more landsliding, its implementation involves important tradeoffs.
71 Insight into such matters is therefore crucial for better catchment management strategies. Yet, there
72 is very little quantitative data on whether the implementation of terraces indeed affects landslide
73 incidence in the tropics and, if so, under which circumstances.

74
75 Hence, the goal of our work is to study the effects of agricultural terraces on landslide incidence
76 in a densely-inhabited tropical landscape. To reach this goal we target the mountainous region of
77 northwestern Rwanda (Africa), a landslide-prone area (Depicker et al., 2020; Dewitte et al., 2021)
78 whose landscape has been reshaped by introducing agricultural terracing (Bizoza, 2011; Kagabo
79 et al., 2013; Rutebuka et al., 2021). More specifically, focusing on recent rainfall-induced landslide
80 events, we investigate the effects of terraces on landslide characteristics (frequency, size, and type)
81 through exploring the role of slope, lithology, and regional landslide susceptibility patterns on their
82 occurrence.

83 **2. Material and Methods**

84 ***2.1. Study area***

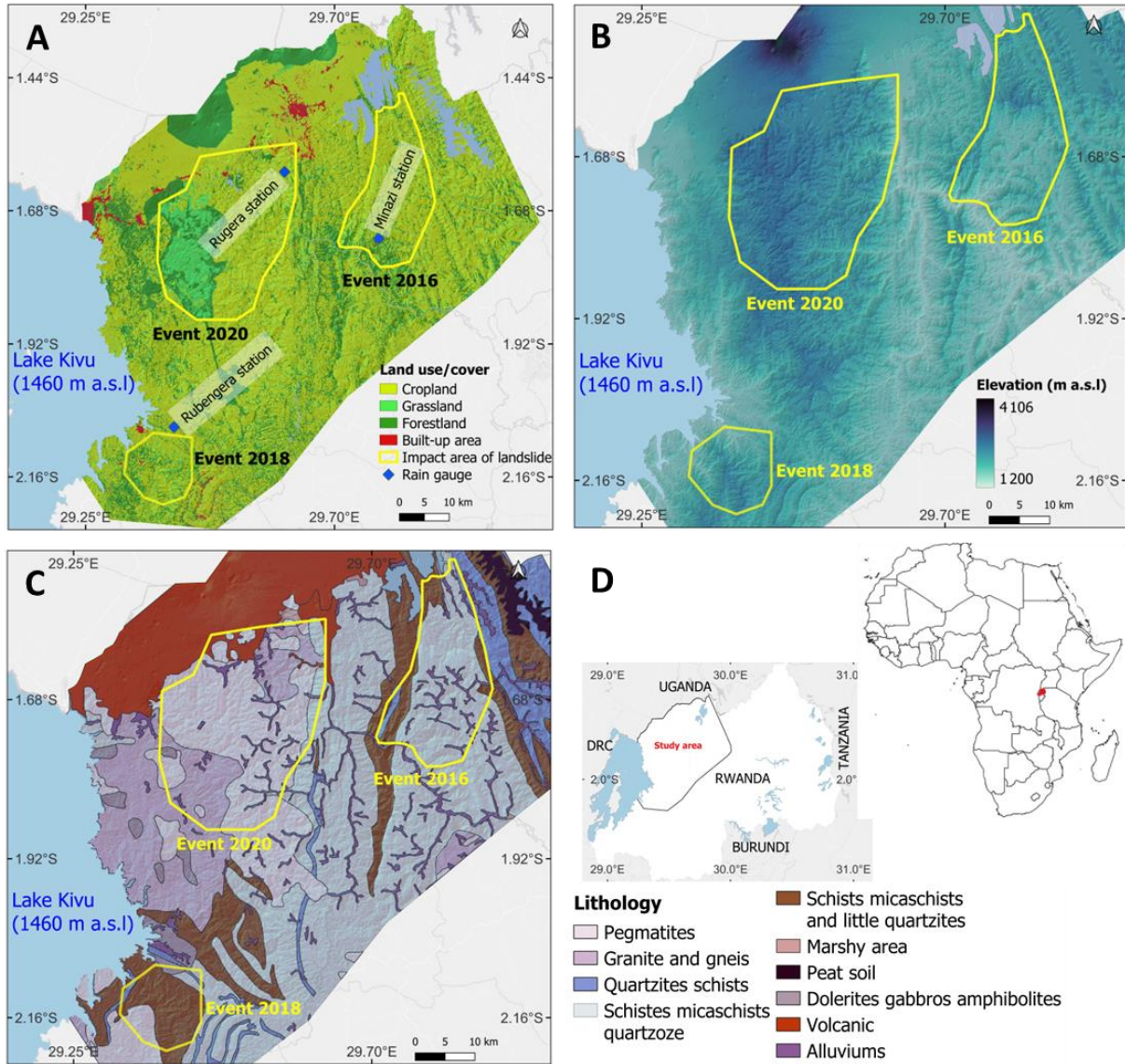
85 Lying within the western branch of the landslide-prone East African Rift (Broeckx et al., 2018;
86 Dewitte et al., 2021; Depicker et al., 2021a), the mountainous landscape of the study area is
87 characterized by a tropical climate with a wet season from September to May and a dry season
88 from June to August, and an average annual rainfall of about 1200 mm (Ministry of Environment,
89 2018). Overall, the susceptibility to landsliding of this landscape (Depicker et al., 2020) is

90 controlled by its steep hillslopes and sometimes deeply weathered lithology (Fig. 1C.) (Depicker
91 et al., 2021a; Dewitte et al., 2021).

92
93 The region is often referred to as the "breadbasket" of the country and is intensely cultivated, with
94 90% of the population involved in agricultural activities (Ministry of Environment, 2018). Its high
95 demographic pressure (~700 inhabitants/km²) and land scarcity result in intensive land use/cover
96 changes through the conversion of forests into agricultural and built-up lands (Nambajimana et al.,
97 2020). This leads to land overexploitation as well as problems of land degradation and soil erosion
98 (Lewis, 1992; Lewis and Nyamulinda, 1996; Roose and Ndayizigiye, 1997; Turkelboom et al.,
99 2008; Kuria et al., 2019). To cope with that problem, agricultural terracing has been promoted as
100 a measure to stabilize soil erosion and enhance land productivity; the implementation of these
101 terraces being particularly intense since 2010 (Bizoza 2011; Kagabo et al., 2013; Rutebuka et al.,
102 2021).

103
104 The common types of terraces in the area are bench, locally called radical, and progressive
105 (forming gradually) terraces (Fig.2). Radical terraces are a series of horizontal or almost horizontal
106 strips running perpendicular to the slope direction at certain vertical intervals, supported by steep
107 risers (Mesfin, 2016). During their construction, workers carefully remove the topsoil to a depth
108 of around 30 cm (Fashaho et al., 2020) and work on the subsoil to create the bench surface
109 (alternating the cut and fill work), after which the topsoil is spread back onto the surface.
110 Generally, those terraces are of a size of between 2 m and 4 m in width, and the riser can reach 2.5
111 m (Fig. 2A, B and C). Stabilization is typically made by planting grass on the vertical face of the
112 riser. Progressive terraces are built with the use of contour bunds, ridges, and ditches made of soil
113 or stones that are placed across the slope direction along the contour. They gradually form over
114 time as a result of erosion, farming activities, and deposition (Mesfin, 2016). Planting grass on the
115 structure creates stability, just like in radical terraces (Van Dijk and Bruijnzeel, 2004; Rutebuka et
116 al., 2021).

117
118
119



120

121

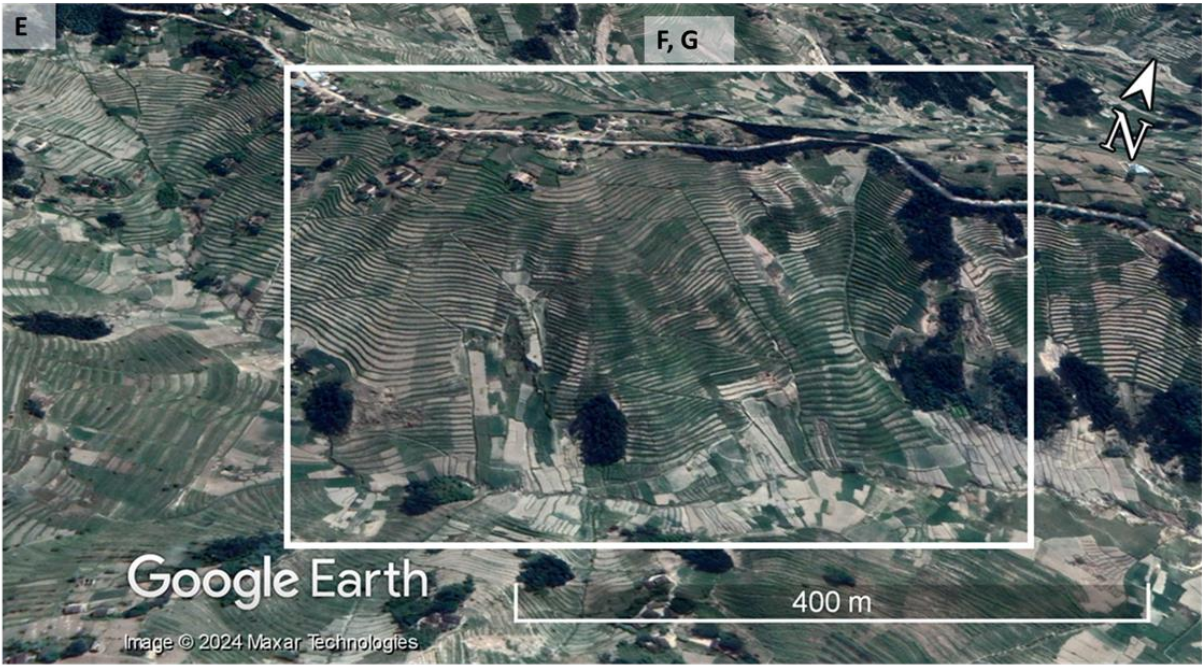
122

123

124

125

Fig. 1: Study area location and characteristics with the delineation of the three clustered zones impacted by the three rainfall-triggered landslide events analyzed in this research (see Section 2.2). **A)** Land use/cover in 2015 based on the Regional Centre for Mapping Resources and Development (RCMRD, 2015). **B)** Elevation based on the Japan Aerospace and Exploration DEM (JAXA, 2010). **C)** Lithology based on the geological map of Rwanda (Theunissen et al., 1991). **D)** Location of the study area.



127 **Fig. 2:** Example of agricultural terraces constructed in the study area. **A)** Radical terraces on pegmatite (picture taken
128 in May 2021; 29°31'25.31"E, 1°40'01.48"S). **B)** and **C)** Radical terraces on quartzites-schists (pictures taken in
129 September 2022; 29°23'24.72"E, 2°10'32.89"S and 29°22'57.30"E, 2°10'18.97"S, respectively). **D)** Progressive
130 terrace on schist-micaschist (picture taken in October 2020; 29°51'15.46"E, 1°29'47.35"S). **E), F)** and **G)** Evolution
131 of a hillslope on pegmatite showing the construction of radical terraces between July 2014 and August 2016
132 (29°31'11.87"E, 1°42'40.85"S); imagery from Google Earth.
133
134

135 **2.2 Landslide events**

136 Our research investigates three rainfall-triggered landslide events that have occurred recently in
137 the study area. These events are relatively important as compared to landslide events that are
138 commonly observed in the East African Rift (Deijns et al., 2024; Niyokwiringirwa, et al., 2024).
139 They are concentrated in three distinct spatial clustered zones (Fig. 1):

- 140 • The first event occurred on May 7 and 8, 2016 in the northern part of the region. According
141 to the government of Rwanda, that event caused 24 deaths, damaged 118 houses and
142 destroyed a large number of crops (MINEMA, 2018).
- 143 • The second event occurred on May 6, 2018 in the southwestern part of the study region
144 (Dewitte et al., 2021; Deijns et al., 2022). This event caused 18 deaths, dozens of injuries,
145 the destruction of 9,974 houses, and the loss of 4.5 km² of crops (Niyonzima, 2018).
- 146 • The third event occurred on May 1, 2020, in the northwestern part of the region and caused
147 28 deaths and the destruction of 450 houses as well as crops.

148 We compared rainfall characteristics associated with the occurrence of the three events based on
149 daily rainfall information obtained from the rain gauges of the Rwanda Meteorological Agency
150 (Meteo Rwanda, 2022) that were closest to each of them (Figure 3). Although uncertainties in
151 rainfall assessment are associated with information at a daily level (Monsieurs et al., 2019) and
152 the location of the rain gauge with respect to the location of the event (Monsieurs et al., 2018a),
153 the use of this rain gauge information is more reliable for landslide event characterization than the
154 use of precipitation products derived from earth observation (Monsieurs et al., 2018b; Nakulopa
155 et al., 2022). We looked at the rainfall amounts on the day of the events and in the 2-day and 12-
156 day periods that precede them. Such rainfall characteristics have been commonly used to study the
157 triggering and antecedent rainfall conditions for landslides that occur outside the tropics (Guzzetti
158 et al., 2007), but their application has also proven to be relevant in the region where our study area
159 is located (Jacobs et al., 2016; Monsieurs et al., 2019; Uwihirwe et al., 2020). This rainfall

160 comparison shows that the events of 2018 and 2020 had overall similar rainfall amounts (Table 1).
 161 Yet, the event of 2016 was characterized by a much higher rainfall depth at the day of the event
 162 (Table 1). The three affected zones also show important contrasts in lithology (Table 2).

163 **Table 1:** Total rainfall amounts in the day(s) before each of the three landslide events, measured at the most nearby
 164 rain gauge station.

Landslide event	Rain gauge station	Rainfall (mm)		
		day of the event	2 days before the event	12 days before the event
2020	Rugera	83	18	159
2018	Rubengera	83	24	188
2016	Minazi	131	11	129

165

166 **Table 2:** Lithology distribution within the clustered zones of the three landslide events (cf. **Fig. 1**). Lithology from
 167 Theunissen et al. (1991).

Lithology	Event 2016	Event 2018	Event 2020
Alluvial deposits	8 %	-	5%
Areas rich in green rocks (dolerite, gabbroas, amphibolites)	-	3%	1%
Granitic and gneissic rocks	-	-	24%
Pegmatite	-	16%	61%
Quartzites dominant on the schistose levels	4%	3%	-
Schists, quartz, micaschist and some quartzitic levels	72%	7%	-
Shales, micaschists and quartzites of little importance	16%	71%	5%
Volcanic rocks	-	-	4%

168

169 **2.3. Constructing the landslide inventories**

170 Visual interpretation of satellite images remains among the most widely used methods to build
 171 detailed landslide inventories that allow accurate characterization of the processes (Guzzetti et al.,
 172 2012; Casagli et al., 2023). A similar approach was followed to map the three rainfall-triggered
 173 landslide events discussed above. Some of the landslides triggered by these rainfalls had already

174 been mapped by Depicker et al. (2021a), Dewitte et al. (2021), and Deijns et al. (2022) through
175 the visual interpretation of very high spatial resolution (< 1m) satellite images available in Google
176 Earth. Here we completed these mapping efforts, making use of additional satellite imagery with
177 similar resolution that was recently made available in Google Earth. The use of Google Earth
178 imagery has been validated with high success to map landslides in the region of the study area
179 (Sekajugo et al., 2022; Maki Mateso et al., 2023; Kanyiginya et al., 2024). On the other hand, the
180 use of automatic classification for landslide inventory does not allow to reach the level of details
181 needed to map the landslides for such an accurate analysis of the processes, especially in complex
182 landscapes disturbed by human activities (Jones et al., 2021; Deijns et al., 2024). Here, in addition
183 to the interpretation of the images, we conducted in-depth field observations and interviews with
184 local residents over the period of February-March 2021 to validate more than 200 of the
185 inventoried landslides, and confirm their time of occurrence.

186

187 Furthermore, we went beyond the simple delineation of the landslide boundaries, adding key
188 landslide characteristics useful for our analyses. These include: determining the time range of
189 available images (typically two to three months after the event's occurrence), and the type of
190 landslides (based on the classification proposed by Hungr et al. (2014)). Furthermore, to better
191 analyze those three landslide events, we manually positioned a point inside the source area of each
192 landslide in order to accurately extract the corresponding environmental settings (e.g., Corominas
193 et al., 2014; Bartelletti et al., 2017; Depicker et al., 2021a; Maki Mateso et al., 2023).

194

195 ***2.4. Controlling factors of landsliding***

196 To link the occurrence and characteristics of the inventoried landslides to the potential presence of
197 terraces, we delineated all terraced areas within each clustered zone of the events on the same
198 satellite images that were used to map the landslides. In doing so, we recorded the type of terrace
199 (i.e., progressive or radical). We assumed a landslide to occur in terraces if its identified source
200 point was located within these mapped terraces.

201

202 We also extracted the hillslope angle of each landslide, which is one of the most important
203 explanatory factors for landslide occurrence (Reichenbach et al., 2018). For this, we used the

204 ALOS PALSAR DEM at a resolution of 12.5 m (JAXA, 2010). This DEM is produced with radar
205 images of 2006-2011, i.e., before the occurrence of the three studied events.

206
207 To have a further idea of the overall likelihood of landslide occurrence, we extracted the landslide
208 susceptibility from a state-of-the-art regional landslide susceptibility map at 30-m resolution that
209 covers our study region (Depicker et al., 2020). The data-driven model behind this map relied on
210 a logistic regression approach and a set of twelve predictors: slope angle, north and east exposure,
211 planar curvature, profile curvature, distance to the drainage network, land cover, lithostratigraphy,
212 distance to active faults, distance to inactive faults, peak ground acceleration (PGA), and the 2-
213 day 15 mm rainfall exceedance. The model was calibrated based on a comprehensive regional
214 historical geomorphological inventory of more than 6,400 landslides of various ages (from recent
215 years to tens of thousands of years), types and depth. The sensitivity of the model was tested
216 against various landslide sampling strategies and successfully validated (with an AUC value for
217 the ROC curve of 0.92; Depicker et al., 2020). As such, by considering a very broad variety of
218 landslide processes associated with the geomorphological evolution of the region (Dewitte et al.,
219 2021), this model represents the long-term landslide susceptibility of the landscape. The landslides
220 of the model of Depicker et al. (2020) are not the landslides used in our study. Although the model
221 uses land cover as a controlling factor, it is important to note that it did not consider the presence
222 of agricultural terraces. As with slope steepness, we used the map to subdivide our study area based
223 on the expected overall landslide susceptibility. For this, we used the original classes as proposed
224 by Depicker et al. (2020). Furthermore, we used the continuous values of the logistic regression,
225 ranging from 0 to 1, to evaluate its performance in predicting the locations of landslides for the
226 three events. Additionally, we explored the potential added value of incorporating the presence of
227 terraces as a predictor, as detailed in Section 2.5.3.

228
229 **2.5. Statistical analyses**

230 **2.5.1. Frequency ratio**
231 To analyze the potential link between landslide occurrence and the presence of agricultural
232 terraces, we calculated the frequency ratios of landslides inside and outside terrace areas. Overall,
233 the frequency ratio (FR) expresses how often landslides occur within a certain class of a potentially

234 controlling factor, controlled for how frequently that class occurs (e.g. Lee and Pradhan, 2007;
 235 Maki Mateso et al., 2023). It was calculated as follows:

$$236 \quad FRi = \frac{nLi/nLs}{Ai/As} \quad (\text{Eq.1})$$

237 where FRi is the frequency ratio for a certain class i of a considered controlling factor ; nLi is the
 238 number of landslides located in class i of the controlling factor; nLs is the total number of
 239 landslides in the study region (S); Ai is the area of i ; and As is the area of the study region. A FRi
 240 > 1 indicates that landslides occur relatively more frequently in i than would be expected based on
 241 the spatial extent of this class.

242 We calculated the landslide density, in terraced and non-terraced areas for different classes of both
 243 slope angle and landslide susceptibility (cf. Section 2.4).

244

245 2.5.2. Odds ratio

246 As an additional measure to quantify the potential effect of terracing on landslide occurrence, we
 247 calculated the odds ratio for landslides occurring in terraced areas vs. landslides occurring in non-
 248 terraced areas. Again, this was done for different classes of slope angle and landslide susceptibility.
 249 The odds ratio (OR) was calculated as follows (Stoltzfus, 2011):

$$250 \quad ORi = \frac{A_T/(1-A_T)}{A_{NT}/(1-A_{NT})} = \frac{A_T \times (1-A_{NT})}{A_{NT} \times (1-A_T)} \quad (\text{Eq.2})$$

251 where ORi is the odds ratio value for a certain class i of a considered controlling factor (e.g., of
 252 slope angle or landslide susceptibility); A_T is the total area of the landside affected area in terraces,
 253 located in class i ; A_{NT} is the total landslide area in non-terraces, located in class i ; $1-A_T$ is the spatial
 254 extent of the non-landslide affected area in terraces; and $1-A_{NT}$ is the spatial extent of the non-
 255 landslide affected area in non-terraced areas. Overall, the OR-value indicates how much more (OR
 256 >1) or less (OR <1) likely it is to find an area affected by landslides in terraced areas as compared
 257 to non-terraced areas.

258

259 2.5.3. Landslide susceptibility

260 It is outside the scope of this paper to predict the exact locations of landslides triggered by the
 261 three considered rainfall events. Nonetheless, our landslide inventories allow to evaluate how well
 262 a state-of-the-art regional landslide susceptibility model by Depicker et al. (2020) (described in
 263 section 2.4) could predict the spatial patterns of these new landslides. For this, we generated a

264 number of non-landslide points in each landslide event cluster. The location of these points was
265 random, except for the fact that they were located at least 30 m away from a mapped landslide
266 polygon. The number of zero points (non-landslide points) was set equal to the number of landslide
267 points (e.g., Depicker et al., 2020). The share of the zero points was determined proportionally to
268 the size of each affected area, which leads to a density of four points per km².

269

270 Using these zero-points as well as the mapped landslide source points, we constructed Receiver
271 Operation Characteristic (ROC) curves for each event as well as the three events combined. ROC
272 curves are a frequently used tool to assess the performance of landslide susceptibility models, with
273 the corresponding Area Under the Curve (AUC) providing an overall metric of the discriminative
274 ability of the model (Broeckx et al., 2018; Reichenbach et al., 2018). We constructed ROC curves
275 for the original model of Depicker et al. (2020). In addition, we explored to what extent the
276 performance of susceptibility models may be improved by incorporating the effect of terraces. For
277 this, we fitted a simple logistic regression model based on two variables: the continuous landslide
278 susceptibility value of the model by Depicker et al. (2020) and a dummy variable, indicating the
279 presence (1) or absence (0) of terraces. Using a susceptibility model output as a predictor variable
280 for another susceptibility assessment is in line with the approach of combining models done by,
281 e.g., Depicker et al. (2020) and Rossi et al. (2010). The terrace variable was derived from our
282 manually mapped terraces, where no further distinction was made between radical and progressive
283 terraces (cf. Section 2.1). Most of the terraces in the three clustered zones have been implemented
284 since 2014-2016. Logistic regressions were fitted in Python, using the *Logistic Regression*
285 functionality of the *sklearn_linear_model* package (Pedregosa et al., 2011).

286

287 *2.5.4. Landslide probability-size distributions*

288 Earlier work demonstrated that sizes and corresponding frequencies of landslides triggered by a
289 certain event such as intense rainfall typically follow a specific inverse-gamma distribution
290 (Malamud et al., 2004). The comparison of such distributions from different landside events allows
291 to understand the importance of natural and human-influenced environmental conditions on their
292 frequency and size (Van Den Eeckhaut et al., 2017; Tanyas et al., 2018; Maki Mateso et al., 2023).
293 To assess to what extent the presence of terraces may affect the sizes of our landslides, we therefore
294 fitted these distributions based on the mapped landslide extents and following the procedure of

295 Malamud et al. (2004). First, we looked at the probability-size distribution for each of the three
 296 landslide events separately. Next, we looked at the probability-size distribution for landslides in
 297 terraced and non-terraced areas separately. Finally, for the 2020 event alone, we looked at
 298 distribution in terraced and non-terraced areas separately.

299

300 **3. Results**

301 **3.1. Landsides inventories**

302 Our inventory contains 4,687 landslides in total. This number corresponds to an extra 2,222
 303 landslides compared to previous inventories compiled by Deijns et al. (2022), Depicker et al.
 304 (2021a), and Dewitte et al. (2021). Most of these landslides are shallow (up to a few meters deep)
 305 avalanches and slides (Hung et al., 2014; Dewitte et al., 2021; Deijns et al., 2024) (**Fig. 3**). The
 306 materials involved were mainly soil and debris. The total area of all the landslides covers
 307 approximately 1% of the areas of the three clustered zones. The largest landslide-affected area is
 308 0.30 km², while the smallest detected landslide is 5 m² and the median size is 522 m².

309 The 2020 landslide event was clearly the largest one, not only in terms of extent of the cluster
 310 zone, but also in terms of the number of landslides, the total landslide area and the number of
 311 landslides on terraces. This event's cluster zone also contains the largest area and proportion of
 312 (mostly radical) terraces. The 2016 event was the smallest in terms of landslide numbers, total
 313 affected area but also the area treated with terraces (**Fig. 3; Table 3**).

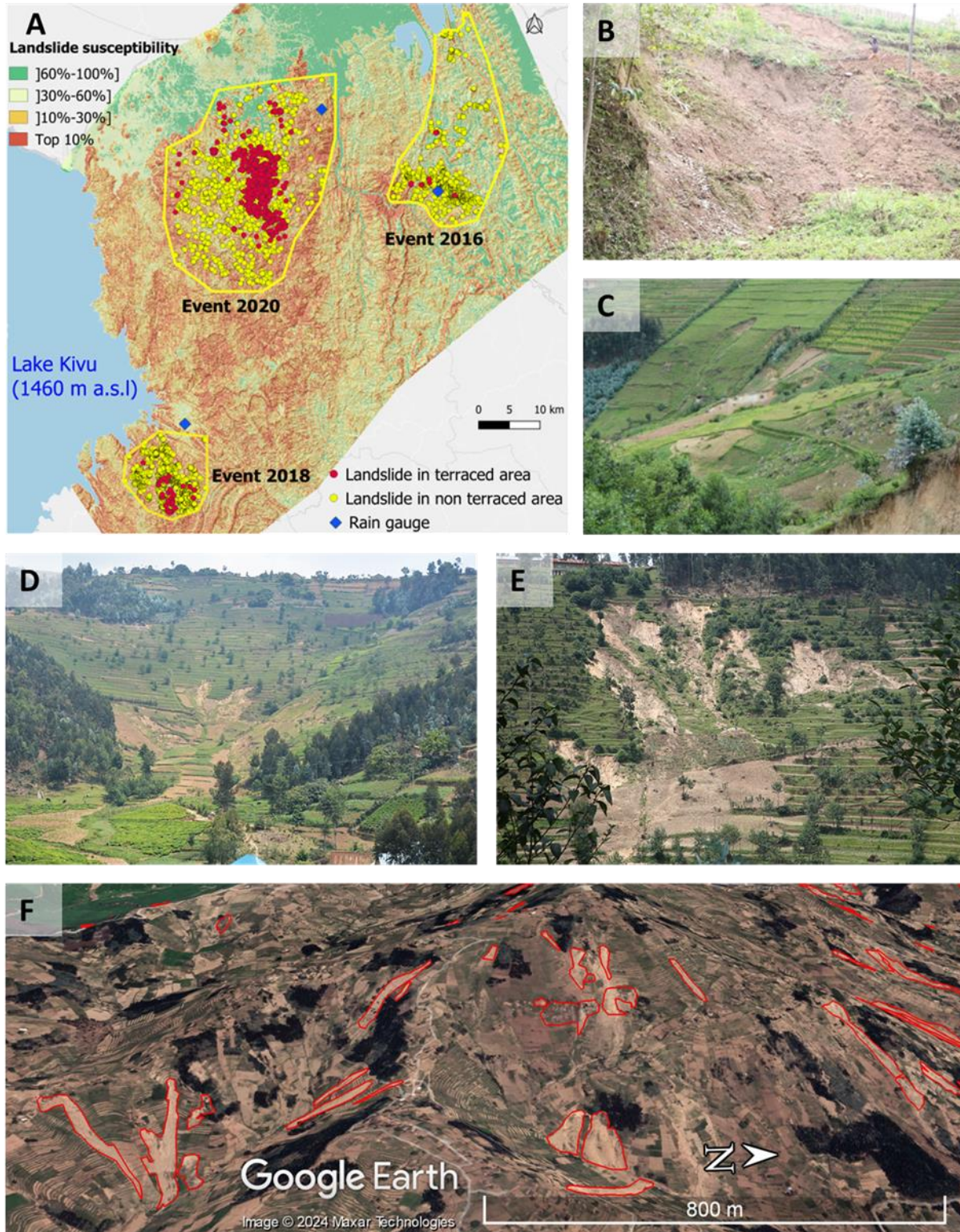
314 **Table 3:** Overview of the inventoried landslides for the three mapped events. ‘#’ stands for number.

Landslide event	Size of event cluster zone (km ²)	Total terraced area (km ²)	Radical terrace area (km ²)	Progressive area (km ²)	Non-terraced area (km ²)	Affected area (km ²)	Total # of landslides	# of landslides on terraces	# of landslides on radical terraces	# of landslides on progressive terraces	# of landslides on non-terraced areas
2020	735.9	73.6	66.2	7.4	662.3	7.2	2,222	709	670	39	1,513
2018	149	9.2	4.2	5	139.6	2.4	1428	50	22	28	1,378
2016	380	6	5.7	0.28	374.5	0.6	1,037	14	9	5	1,023
All	1,265	88.8	76.1	12.7	1,176.4	10.2	4,687	773	701	72	3,914

315

316

317



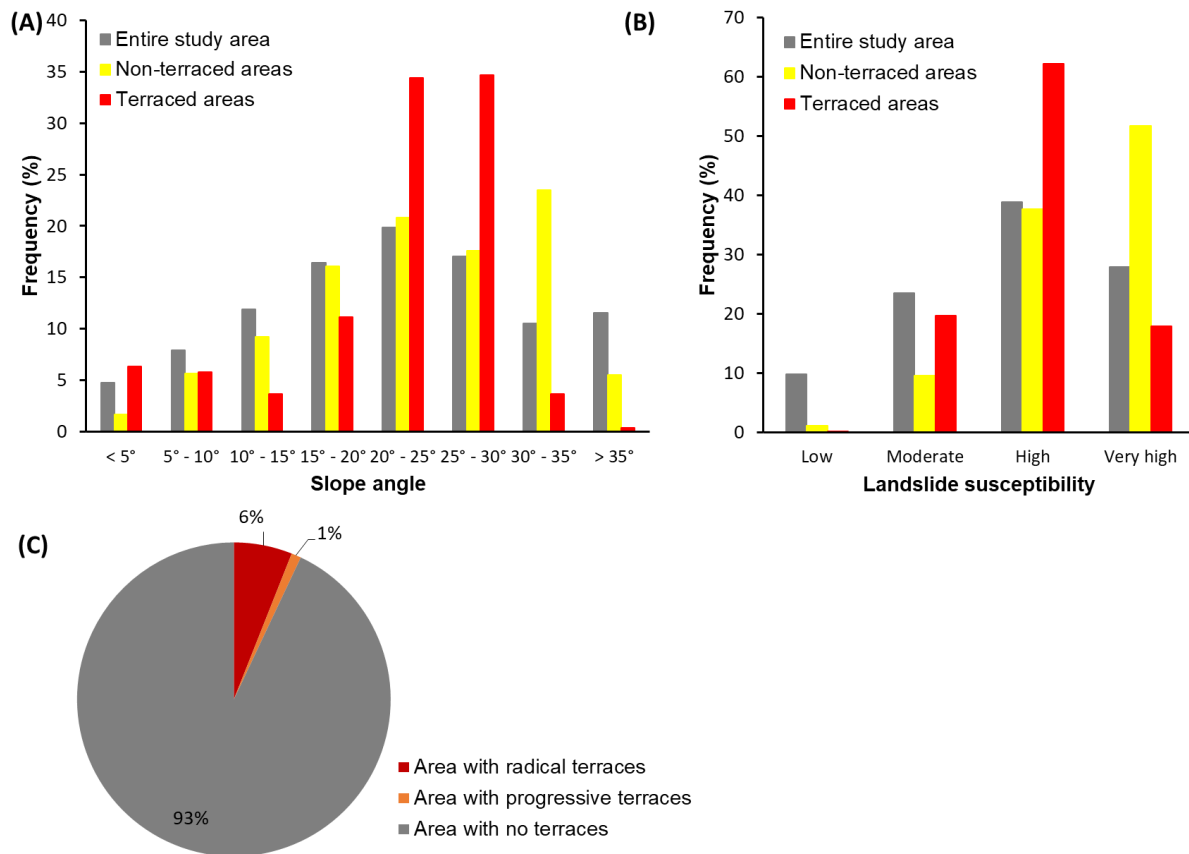
318

319 **Fig. 3:** Landslide inventory and some examples. (A) distribution of landslides triggered by the three events. The
 320 background shows the expected landslide susceptibility (Depicker et al., 2020). Four classes of susceptibility were
 321 provided as follows: the top 10% (here qualified as very high susceptibility), the 10%-30% (high susceptibility), the
 322 30%-60% (moderate susceptibility), and the 60%-100% (low susceptibility). (B) Landslide in a cultivated, non-
 323 terraced hillslope (picture taken in October 2020; 29°45'26.15"E, 1°35'23.92"S). (C) Landslides in progressive

terraces (picture taken in October 2020; 29°31'48.63"E, 1°44'36.923S). (D) and (E) Landslides in radical terraces (pictures taken in October 2020; (D): 29°31'33.14"E, 1°40'10.71"S; (E): 29°30'13.45"E, 1°38'32.83"S). (F) Several landslides of the landslide event of 2020 as mapped on an image of August 2020 from Google Earth (29°31'1.63"E, 1°45'18.32"S).

3.2. Effect of terracing on landslide occurrence

Considering all three event clusters together, agricultural terraces cover only around 7% of the study area (Fig. 4). Nonetheless, a disproportionately large amount of landslides that were mapped across these three events occurred in terraces. This is true in terms of frequency ratio, as well as in terms of odds ratios (Fig. 5a). For the three events combined, the odds ratio indicates that landslides were about three times as likely to occur in terraced areas as compared to non-terraced areas.



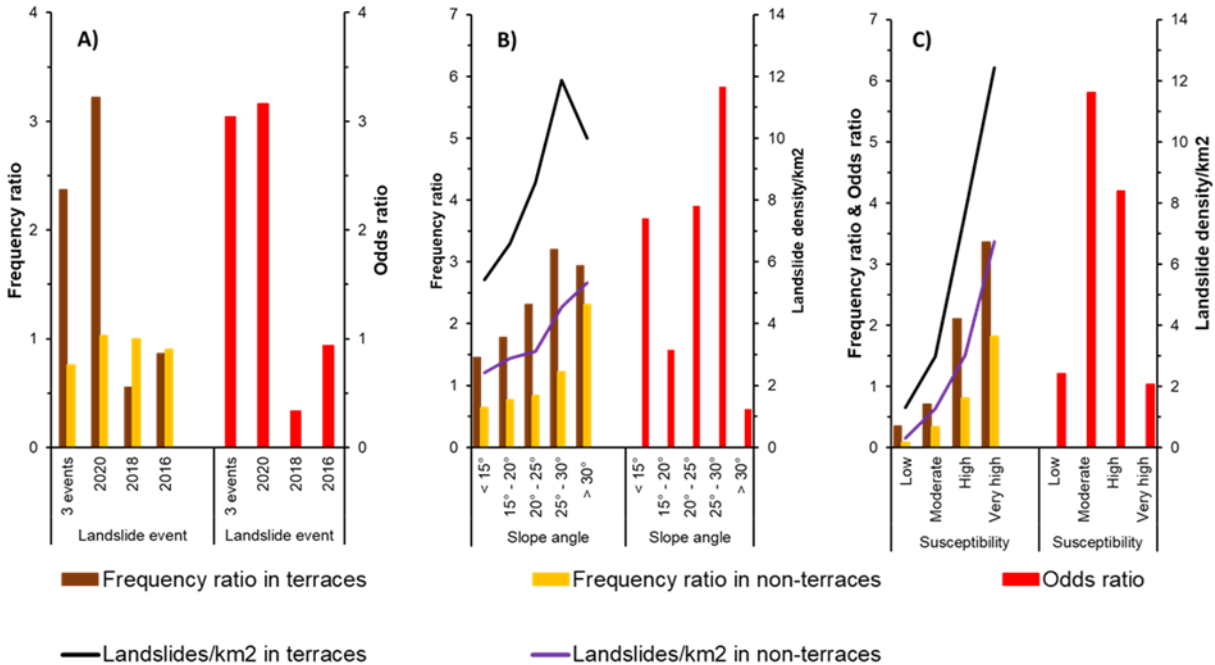
336
337 **Fig. 4:** Characterization of the three landslide events combined. (A) Frequency distributions of slope angles within
338 the study area, subdivided in terraced and non-terraced areas. (B) Frequency distributions of landslide susceptibility
339 classes within the study area (as defined by Depicker et al., 2020), subdivided in terraced and non-terraced areas. (C)
340 Frequency distribution of areas with radical terraces, progressive terraces, or no terraces.
341

342 First, large contrasts exist between the three events. For the event of 2020, which was the overall
343 largest event that occurred in an area with the highest proportion of terraces (**Table 3**), the odds
344 ratio was 3.2 (**Fig. 5A**). Yet, for the 2018 event, the odds ratio was only 0.34, indicating that
345 landslides were three times less likely to occur in terraces as compared to non-terraced areas. For
346 the 2016 event, the odds ratio is close to one, suggesting no clear effect. However, with only ~1.6%
347 of the area covered by terraces and only 14 landslides recorded in these terraces (**Table 3**), this
348 value may be little representative.

349

350 Considering the landslide occurrence per slope angle class (**Fig. 5B**), landslide densities and
351 frequency ratios generally increase with slope steepness. This holds for both terraced and non-
352 terraced areas. Nevertheless, both terraced and non-terraced areas tend to show a different trend in
353 terms of landslide occurrence, which is also reflected in the odds ratios. For relatively flat areas ($<$
354 15°), landslides were about 3.5 times more likely to occur in terraced as compared to non-terraced
355 areas. However, given the overall low frequency of landslides in this slope class (**Fig. 4A**), this
356 result should be interpreted with caution. For moderate slope classes, the odds ratio starts around
357 1.5 (15° - 20°) but then strongly increases to nearly six (25° - 30°). However, for steeper slope classes
358 ($> 30^\circ$), the odds ratio drops below one. While many landslides fall within this slope class, the
359 extent of terraces in areas steeper than 30° is limited (**Fig. 4A**). Overall, these results indicate that
360 the relatively higher occurrence of landslides in terraced areas mainly occurs in areas with a gentle
361 to moderately steep slopes ($< 30^\circ$).

362



363
 364 **Fig. 5:** Frequency ratios, odds ratios, and landslide frequencies for the three landslide events combined: (A) per
 365 landslide event; (B) three events combined, subdivisions per slope class; and (C) for the three events combined,
 366 subdivided per landslide susceptibility class.

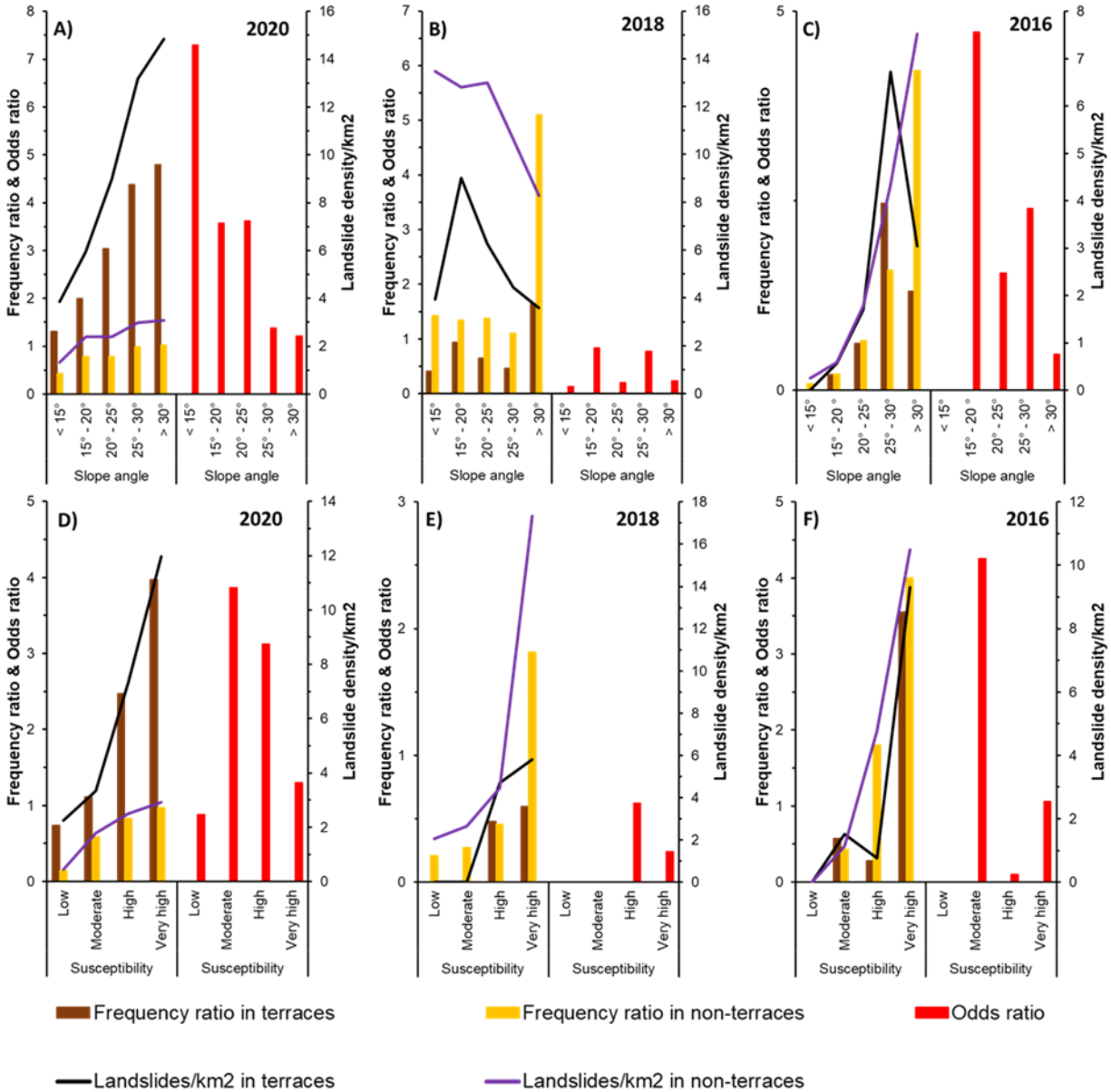
367
 368 Comparable results can be found when considering landslide susceptibility (**Fig. 5C**). As can be
 369 expected, landslide frequency ratios and densities strongly increase with the susceptibility class in
 370 both terraced and non-terraced areas. However, the contrast between both is especially pronounced
 371 for areas with a moderate to high susceptibility (with odds ratios ranging between 4 and 6). In
 372 areas with a very high susceptibility, the odds ratio lies close to one. The same holds for areas with
 373 a low susceptibility. Yet, in this case, also the number of landslides is overall very limited (**Fig.**
 374 **4B**).

375
 376 **Fig. 6** presents a further exploration of these trends, separated per event. For the 2020 event, results
 377 are relatively similar to the overall analyses (**Fig. 5**), which is to be expected as this event also
 378 contributes the largest number of landslides and terraced areas to the combined dataset (**Table 3;**
 379 **Fig. 3**). Again, the effect of terracing on landslide occurrence is largest for weak to moderate
 380 slopes, with odds ratios dropping to around 1 for slopes steeper than 25° (**Fig. 6A**). In terms of
 381 landslide susceptibility, the odds ratios for landslides on terraced versus non-terraced areas are

382 clearly higher for moderately to highly susceptible zones (**Fig. 6D**). Yet, for areas with a low and
383 very high susceptibility, the difference is clearly much less pronounced.

384

385 Clearly different patterns emerge for the 2018 event. Frequency ratios generally do not increase
386 greatly with slope angle, except for slopes steeper than 30° (**Fig. 6B**). Across all these slope classes,
387 frequency ratios and landslide densities are lower in terraced than in unterraced areas, resulting in
388 odds ratios below one. For this event, no landslides occurred in terraced areas with a low to
389 moderate susceptibility (**Fig. 6E**). Yet, for areas with high to very high susceptibilities odds ratios
390 are also clearly below 1. For the 2016 event, landslide frequencies and densities generally increase
391 with both slope angle (**Fig. 6C**) and landslide susceptibility (**Fig. 6F**). As for the 2020 event, odds
392 ratios are generally larger than one for areas with a moderate slope angle (15° - 20°), but drop for
393 slopes $>30^\circ$ (**Fig. 6C**). Likewise, odds ratios are higher for areas with a moderate susceptibility
394 (**Fig. 6F**). However, given the limited extent of terraced areas in this event zone and since only 14
395 landslides were mapped in these terraces (**Table 3**), these results should be interpreted with
396 caution.



397

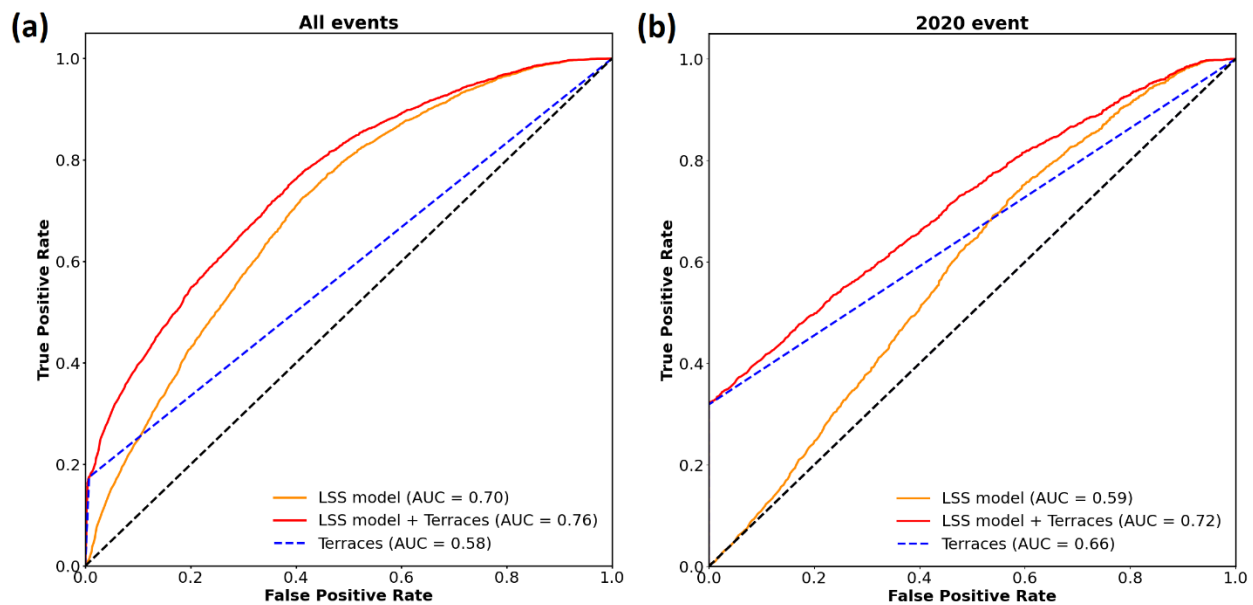
398 **Fig. 6:** Frequency ratio, landslide density, and odds ratios of landslides on terraced versus non-terraced areas for the
 399 three separate events. (A), (B), and (C) show these metrics per slope class for respectively the 2020, 2018 and 2016
 400 events. (D), (E), and (F) shows the same metrics per class of landslide susceptibility for respectively the 2020, 2018
 401 and 2016 events.

402 3.3. Potential effect of terraces on landslide susceptibility

403 The earlier developed regional landslide susceptibility model by Depicker et al. (2020) performs
 404 overall relatively weakly in predicting the source locations of the landslides triggered by the
 405 rainfall events (**Fig. 7**). Constructing a Receiver Operation Characteristic (ROC) Curve based on
 406 this model for the three events combined results in an Area Under the Curve (AUC) of only 0.62

407 (Fig. 7a). Especially for the 2020 event, the model could not well discriminate the landslide from
408 non-landslide areas (Fig. 7b). For the 2018 and 2016 events, the model performed better with AUC
409 values of respectively 0.75 and 0.82.

410 When we add the presence (1) or absence (0) of terraces as a dummy variable to the existing model
411 by Depicker et al. (2020), the predictive accuracy of landslide locations triggered by the events
412 seems to be clearly improved (Fig. 7a). This is particularly so for the 2020 event, where including
413 this dummy variable increases the AUC value to 0.72. For the other two events, adding this dummy
414 variable led only to marginal improvements (with changes in AUC value of less than 0.01).



415

416 **Fig. 7:** Receiver Operation Characteristic (ROC) curves for the landslide susceptibility (LSS) model of Depicker et
417 al. (2020), for all three events (a) and for the 2020 event (b). Yellow lines show the ROC curve based on the original
418 model with the Area Under the Curve (AUC) value indicated in the legend. Blue lines show the ROC curve when only
419 a dummy variable indicating the presence or absence terraces would be used. Red lines show the ROC curve based on
420 the LSS model plus this dummy variable.

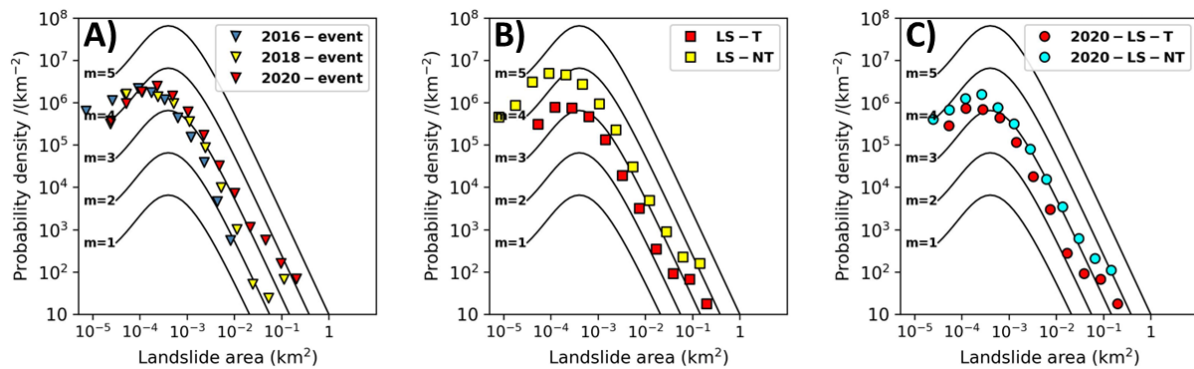
421 3.4. Size-frequency distribution

422 All three events show a size-frequency distribution (Fig. 8A) that matches relatively well with the
423 gamma distribution proposed by Malamud et al. (2004). Yet, with landslides of around 100 to
424 1000 m² occurring most frequently, the ‘rollover’ in size-frequency distribution occurs at slightly
425 smaller sizes than the theoretical distribution would suggest. This indicates that a relatively high
426 number of small landslides occurred. Overall, the three events show different size-frequency

427 distributions (Kruskal-Wallis test $p < 0.000$). Moreover, the 2020 event tends to have a higher
428 frequency of larger landslides ($> 10,000 \text{ m}^2$; **Fig. 8A**) and greater variability.

429 Considered over the three events combined, landslides in non-terraced areas tend to have a slightly
430 higher size-frequency distribution than landslides in terraces (**Fig. 8B**). The same holds for the
431 2020 event, indicating that landslides occurring in terraces tend to be typically slightly smaller
432 (**Fig. 8C**). For the other two events, the number of landslides occurring in terraces was too low to
433 fit a separate size-frequency distribution (**Table 3**).

434



435

436 **Fig. 8:** Landslide size-frequency distribution for (A) the three mapped landslide events; (B) all mapped landslides
437 across the three events that occurred in terraced and non-terraced areas; and (C) the 2020 landslide event, subdivided
438 for terraced and non-terraced areas. LS-T: landslides in terraced areas, LS-NT: Landslides in non-terraced areas. The
439 theoretical distributions for various landslide-event magnitudes (m) proposed by Malamud et al. (2004) are
440 represented with black curves. An inventory that that would contain 100 landslides is represented by $m = 2$; 1000
441 landslides by $m = 3$, etc.

442

443 4. Discussion

444 4.1. A highly landslide-prone region

445 Several earlier studies already highlighted the significance and dangers of rainfall-triggered
446 landsliding in tropical hilly and mountainous regions like NW Rwanda (e.g., Monsieurs et al.,
447 2018; Depicker et al., 2020; Dewitte et al., 2021; Depicker et al., 2021b; Deijns et al., 2022). With
448 over 4,600 landslides mapped across the three studied events, our results further demonstrate this
449 importance (**Fig. 3; Table 3**). All three events occurred in May, which corresponds to the end of
450 the second rainy peak of the wet season and is generally the period with the highest landslide
451 activity in the region (Monsieurs et al., 2018). It is at such moments, when soil moisture contents
452 have already built up to very high levels, that large but not necessarily exceptional rainfall events
453 (**Table 1**) can have devastating impacts (Monsieurs et al., 2018a).

454

455 Most of the landslides mapped were shallow landslides of the avalanche or slide type affecting soil
456 and debris material; i.e., two types of landslide processes of different mobility behaviors that
457 frequently interact and that are commonly associated with intense short-duration rainfall events
458 (Hung et al., 2014). This was clear from the interpretation of the Google Earth imagery and further
459 confirmed by our field surveys. It also corresponds to the findings of earlier research in the region
460 (e.g., Monsieurs et al., 2018; Depicker et al., 2020, 2021a; Dewitte et al., 2021; Deijns et al., 2024)
461 and other places in the African Rift for example (Niyokwiringirwa et al., 2024). Our analyses (**Fig.**
462 **8**) further indicate that the observed landslides are often relatively small, with a rollover in size-
463 frequency distribution occurring around 100 m². This is likely attributable to the often relatively
464 shallow depth of the shear plane (Depicker et al., 2021a). Remarkably, landslides mapped on
465 terraces tend to be slightly smaller than those mapped in non-terraced areas (**Fig. 8B, 8C**). This
466 could indicate that some of the observed landslides in terraces may in fact be caused by local
467 oversteepening and/or collapse and/or overloading at terrace risers (Critchley and Bruijnzeel,
468 1995; Tarolli et al., 2014).

469

470 **4.2. Contrasts between the events**

471 Considered over the three events combined, landslides appear to be around three times as likely to
472 occur in terraced areas than in non-terraced areas (**Fig. 5**). This is in line with the findings of earlier
473 studies in other regions (Crosta et al., 2003; Turkelboom et al., 2008; Cevasco et al., 2013;
474 Agnoletti et al., 2018). Yet, our results provide some of the first quantitative evidence for this from
475 a tropical region in Africa (Kitutu et al., 2011).

476

477 Nevertheless, our results also demonstrate the complexity of rainfall-triggered landsliding in
478 terraced tropical landscapes. For example, of the three events studied, only the 2020 event showed
479 a very clear impact of terracing on landslide occurrence (**Fig. 5A**). Noteworthy, this was also the
480 most significant event, both in terms of landslides triggered and terraced areas (**Table 3**). For the
481 2018 event, however, landslides tended to occur less frequently in terraced than on non-terraced
482 areas, while no clear terrace-effect could be detected for the 2016 event. Yet, for this last event,
483 also the extent of terraces in the affected area was very limited (**Table 3**).

484

485 Several factors and mechanisms may help explaining why landslides occurred much more
486 frequently in terraces during the 2020 event. First, as already indicated above, the construction of
487 terraces may lead to oversteepening and overloading. This, in combination with the local
488 heterogeneities in soil strength that the construction of terraces may induce (Crosta et al., 2003;
489 Milledge et al., 2014) can result in overall lower slope stabilities. Second, terraces can significantly
490 alter the water balance of hillslopes. By design, terraces aim to limit runoff and promote
491 infiltration, which can lead to soil saturation and increased failure risks (Crosta et al., 2003; Brown
492 et al., 2021). This is especially so near the riser of terraces where the local hillslope is steepest,
493 much of the soil water accumulates and the increased soil thickness is potentially larger than the
494 rooting depth of the vegetation (Arnáez et al., 2015; Pijl et al., 2021).

495
496 Nevertheless, it remains unclear why the 2018 event showed overall lower odd ratios for landslides
497 triggered on terraces as compared to non-terraces (**Fig. 5; 6**). Both the 2018 and 2020 events were
498 clearly significant in scale (**Fig. 3**) and were associated with rainfall amounts that look similar
499 (**Table 1**). In addition, the terraces are all being used and relatively well-maintained in both areas;
500 hence, terrace abandonment cannot be invoked as a cause of increased landslide incidence in the
501 2020 event (Crosta et al., 2003; Pepe et al., 2019).

502
503 One element that may play a role is the underlying lithology and the regolith and soil characteristics
504 that result from this. The area affected by the 2018 event is mainly dominated by shales,
505 micaschists, and schists, which can be expected to mainly result in clayey weathering products
506 (**Table 2**). The 2020-event area, on the other hand, is mainly characterized by pegmatite, granite
507 and gneiss (**Table 2**), which often weather into sandier soil types. As sandy soils tend to be more
508 permeable and less cohesive (Das, 2010; Thomas et al., 2020), it may be possible that the impact
509 of terraces on landsliding is more pronounced on sandy hillslopes. Terraces have the capacity to
510 ameliorate soil moisture content by altering the hydrological dynamics of the soil. On sandy
511 hillslopes, this phenomenon might reduce the shear strength of the soil, therefore increasing its
512 potential to instability (Sasahara and Sakai, 2014; Terajima et al., 2014). Yet, further analyses
513 revealed no clearly interpretable differences in odds ratios when grouping landslide occurrence per
514 lithology. This may be attributable to the lack of sufficiently detailed soil and lithology maps, as
515 well as to the role of other confounding factors. For example, small-scale variations in soil

516 characteristics will also affect land use and vegetation patterns, which in turn may influence
517 hillslope hydrology and landsliding. Likewise, differences in landslide occurrence within the
518 affected areas may be strongly influenced by local variations in rainfall conditions during the event
519 (Monsieurs et al., 2018; 2019). However, also here, we lacked sufficiently detailed information to
520 further analyze this. Another potentially important element is that relatively more progressive
521 terraces occur in the area affected by 2018 event, while the 2020 event mainly occurred in an area
522 with radical terraces (**Table 3**). Given their much more limited effect on slope morphology (**Fig.**
523 **2**), it may be expected that progressive terraces will have a smaller impact on landslide dynamics.
524 Nonetheless, no strong contrasts in frequency ratios could be observed for both terrace groups.
525 Furthermore, this would only explain why we would see a less clear impact of terraces; not why
526 relatively less landslides occurred in terraces for the 2018 event.

527

528 As such, our findings also indicate the limitations of geostatistical analyses to understand the effect
529 of terracing on rainfall-triggered landsliding. Despite their added value, such broadscale analyses
530 are best also complemented with more detailed field-based and process-oriented research. In
531 particular, actual observations on the relation between soil moisture in relation to rainfall, soil
532 characteristics and land use/management practices would provide an important added value here.
533 Yet, despite recent advancements (e.g., Thomas et al., 2019, 2020; Wicki et al., 2021; Uwihirwe
534 et al., 2022), such observations remain very rare for the tropical Global South; in particular when
535 it comes to the role of terraces (Sidle et al., 2006; Lewis et al., 2015; Wei et al., 2016).

536

537 ***4.3. Terraces and landslide susceptibility***

538 Despite the difficulties to fully explain the contrasts in results across the three events, our findings
539 clearly demonstrate that the increased likelihood of landslides in terraced areas mainly occurs on
540 hillslopes with a moderate to high landslide susceptibility. The effect is much less pronounced for
541 areas already having a very high susceptibility (**Fig. 5C**). This is certainly the case for the 2020
542 event (**Fig. 6D**), but also for the other two events, odds ratios tend to be relatively lower in very
543 susceptible areas (**Fig. 6E, 6F**). Similarly, odd ratios tend to be higher for moderate to steep slopes
544 (15-30°), but lower for very steep slopes (> 30°; **Fig. 5B**). To some extent, this may be linked to
545 the fact that terraces are also much less frequently constructed on very steep hillslopes (**Fig. 4**),
546 i.e. on the slopes that are characterized by the highest landslide susceptibility (Depicker et al.,

547 2020). Even with terraces, these slopes often remain less suitable for cultivation. This is in
548 confirmation with Water for Growth Rwanda (2018) who reported that in Rwanda, they construct
549 agricultural terraces on hillslopes with a specific slope angle, typically below 35°. The slopes in
550 the class > 30° coincide with the presence of threshold hillslopes; i.e. slope angle conditions that
551 are associated with a clear increase of landslide activity (Depicker et al., 2021a). Moreover, it is
552 mainly on these already susceptible but not extremely landslide-prone hillslopes that terraces can
553 be expected to make an important difference. It is mainly there that small changes in shear stress
554 or strength, for example due to increased soil moisture contents or local oversteepening, can tip
555 the balance towards unstable hillslope conditions (e.g., Schilirò et al., 2018).

556

557 This also has important implications for landslide prediction. Earlier work already indicated that
558 uncertainties on predicted landslide occurrences are overall largest in areas with a moderate
559 estimated susceptibility (e.g., Rossi et al., 2010; Broeckx et al., 2018). While the most and least
560 susceptible areas are often easy to determine, it is in this range of moderately susceptible hillslopes
561 that small changes in hillslope conditions can make a significant difference. This is also
562 demonstrated by the comparison of our landslide inventories with the regional landslide
563 susceptibility map of Depicker et al. (2020) (**Fig. 7**). While this map could somewhat predict where
564 landslides were to be expected in the three impact zones, the performance is overall much lower
565 than the original validation result (with a validation AUC of 0.92; Depicker et al., 2020). This is
566 especially so for the 2020 event, where the map performs only slightly better than a random model.
567 Several elements may explain this. For example, the model of Depicker et al. (2020) was trained
568 at the regional scale level on a variety of landslides types in different geomorphological and
569 lithological contexts, occurring over much longer periods that faced different climate conditions
570 (Dewitte et al., 2021). The model of Depicker et al. (2020) is also not accounting for particular soil
571 and conservation practices as land use controlling factor. Furthermore, as already indicated above,
572 landslide patterns within the affected zone were likely greatly influenced by local rainfall
573 conditions. The exact rainfall patterns were unknown and uncounted for by this susceptibility
574 model. Yet, it is known that such variations can be very significant in tropical environments (e.g.,
575 Monsieurs et al., 2017; 2018).

576

577 Nevertheless, our results indicate that landslide susceptibility models in this region could greatly
578 improve their predictive performance by accounting for the effect of terraces. This is especially
579 the case for the 2020 event (**Fig. 7b**), where a simple dummy variable indicating the presence or
580 absence of terraces was already better in discriminating in landslide from non-landslide areas than
581 the model by Depicker et al. (2020). Yet, as in many regions, systematic data on the presence and
582 characteristics of terraces are lacking for this part of the world.

583

584 ***4.4. Implication for land management and soil and water conservation strategy***

585 Given that terracing mainly occurs on hillslopes with a moderate to high landslide susceptibility
586 (**Fig. 4**), our findings also illustrate the difficulty of developing appropriate land management
587 strategies in mountainous and intensely cultivated tropical regions like NW Rwanda. Given the
588 high slope gradient of many cultivated plots (e.g., **Fig. 3**), terraces are often a requirement for
589 cultivation and can be expected to be an effective strategy to reduce soil erosion (e.g., Ehabu et
590 al., 2022). Yet, these terraces can in some situations significantly increase the landslide risk. As
591 our results illustrate, these risks remain difficult to predict. For example, they are not necessarily
592 only the most susceptible zones that should be safeguarded from terracing. Furthermore, not every
593 rainfall-triggered landsliding event will result in higher landslide rates on terraces. Nonetheless, as
594 the results for the 2020 event demonstrate (**Fig. 5, 7**), terraces can in some cases drastically
595 increase the occurrence of landsliding.

596

597 Various studies already indicated that especially the abandonment and poor maintenance of terrace
598 can result in elevated landslide risks (e.g., Cammeraat, 2004; Koulouri and Giourga, 2007; Romero
599 Díaz et al., 2007; Lesschen et al., 2008; García-Ruiz et al., 2013; LaFevor, 2014; Arnáez et al.,
600 2015; Londoño et al., 2017; Chen et al., 2023). Yet, it is important to note that the terraces in our
601 study area were not abandoned and overall well-maintained. In addition, the rainfall events
602 associated with our events were clearly significant, but, as showed by Monsieurs et al. (2018a) not
603 exceptional (**Table 1**). This further indicates that the higher occurrence of landslides on terraces
604 cannot be attributed to extreme circumstances or poor maintenance, but intrinsically linked to the
605 presence of terraces themselves.

606

607 As such, under the high population pressure that Rwanda is facing, choosing between the potential
608 for cultivation, reduced erosion risks, or reduced landslide risks can become a very difficult
609 exercise. The relevance of making this tradeoff correctly and of finding ways to further minimize
610 landslide risks will likely only increase in the future (Depicker et al., 2021b). While agricultural
611 terraces have already been constructed at a large scale in NW Rwanda (e.g., Bizoza, 2011; Uwacu
612 et al., 2021), their extent will likely continue to increase in the near future.

613

614 **5. Conclusion**

615 Based on the analyses of three rainfall-triggered landslide events in NW Rwanda, we showed that
616 terracing can overall lead, in this specific case, to around three times more landslides as compared
617 to non-terraced areas. While this finding is overall in line with findings from other studies, this
618 work is to our knowledge the first, large-scale quantitative demonstration of this effect for tropical
619 Africa; a region facing enormous land use pressure and likely an important future increase in
620 terraces.

621

622 Yet, our work also demonstrates the large variability and complexity of assessing landslide
623 occurrence in relation to terracing. First, the largest 2020 landside event, which also features >
624 80% of the terraced areas of our study, clearly demonstrated the impact of terracing on landsliding.
625 For the other two events, no (2016 event) or even a negative (2018 event) effect was observed.
626 Yet, the much lower extent of terraces in these two affected regions makes it difficult to draw hard
627 statistically supported conclusions from this. Second, increased landsliding due to terracing was
628 mainly observed on hillslopes with a moderate to high landslide susceptibility and less so on very
629 susceptible slopes. Not only are these moderately susceptible slopes more frequently terraced, it is
630 likely also here that changes in hillslope hydrology induced by the terraces have the largest effect.
631 Third, while more frequent, landslides occurring in terraces tend to be slightly smaller.

632

633 These findings have important implications for land management and soil and water conservation
634 strategy, as they demonstrate that finding a tradeoff between allowing agriculture, reducing soil
635 erosion and reducing landslide risks can present a very difficult exercises. Our results open
636 promising perspectives here as they demonstrate that incorporating the presence of terraces in

637 landslide susceptibility models can lead to more accurate predictions. Nonetheless, geo-statistical
638 analyses as presented in this work also come with limitations. More research is therefore
639 recommended to further disentangle the relationships between terracing and landsliding,
640 particularly in such tropical environments where knowledge on soil and climate remains limited.
641 Especially field-based observations on the relationship between rainfall patterns and soil moisture
642 under contrasting land management practices and soil types can likely shed more light on the
643 complexities revealed by our results.

644

645 **Acknowledgements**

646 The Académie de Recherche et d'Enseignement Supérieur (ARES), in collaboration with the
647 University of Liège (ULiège), the Royal Museum for Central Africa (RMCA), the University of
648 Namur (UNamur), the University of Rwanda, Rwanda Polytechnics, and INES-Ruhengeri,
649 financially supported this work through the research and development project "Landslide and flood
650 hazards and vulnerability in NW Rwanda: towards applicable land management and disaster risk
651 reduction" (LAFHAZAV). Many thanks to Meteo Rwanda, which provided the rainfall dataset.
652 We also thank the National Council for Science and Technology (NCST) of Rwanda for its
653 facilitation of the field data collection process. Finally, we express our gratitude to the reviewers
654 and the editor for their help in improving the content and readability of the paper.

655

656 **References**

- 657 Agnoletti, M., Errico, A., Santoro, A., Dani, A., Preti, F., 2019. Terraced landscapes and
658 hydrogeological risk. Effects of land abandonment in Cinque Terre (Italy) during Severe
659 rainfall events. *Sustainability*, 11, 235. <https://doi.org/10.3390/su11010235>
- 660 Al Qudah, K., Abdelal, Q., Hamarneh, C., Abu-Jaber, N., 2016. Taming the torrents: the
661 hydrological impacts of ancient terracing practices in Jordan. *Journal of Hydrology*, 542,
662 913-922. <http://dx.doi.org/10.1016/j.jhydrol.2016.09.061>
- 663 Amsalu, A., de Graaff, J., 2006. Farmers' views of soil erosion problems and their conservation
664 knowledge at Beressa watershed, central highlands of Ethiopia. *Agriculture and Human
665 Values*, 23(1), 99–108. <https://doi.org/10.1007/s10460-005-5872-4>
- 666 Arnáez, J., Lana-Renault, N., Lasanta, T., Ruiz-Flaño, P., Castroviejo, J., 2015. Effects of farming
667 terraces on hydrological and geomorphological processes. A review. *Catena*, 128, 122–
668 134. <https://dx.doi.org/10.1016/j.catena.2015.01.021>
- 669 Bartelletti, C., Giannecchini, R., D'Amato Avanzi, G., Galanti, Y., Mazzali, A., 2017. The
670 influence of geological-morphological and land use settings on shallow landslides in the
671 Pogliaschina T. Basin (northern apennines, Italy). *Journal of Maps*, 13(2), 142–152.
672 <https://doi.org/10.1080/17445647.2017.1279082>

- 673 Bizoza, A. R., 2011. Farmers, institutions and land conservation: institutional economic analysis
674 of bench terraces in the highlands of Rwanda. (Unpublished doctoral thesis) at Wageningen
675 University, Netherlands
- 676 Broeckx, J., Vanmaercke, M., Duchateau, R., Poesen, J., 2018. A data-based landslide
677 susceptibility map of Africa. *Earth-Science Reviews*, 185(2017), 102–121.
678 <https://doi.org/10.1016/j.earscirev.2018.05.002>
- 679 Brown, A. G., Fallu, D., Walsh, K., Cucchiaro, S., Tarolli, P., Zhao, P., Pears, B. R., van Oost, K.,
680 Snape, L., Lang, A., Albert, R. M., Alsos, I. G., Waddington, C., 2021. Ending the
681 Cinderella status of terraces and lynchets in Europe: The geomorphology of agricultural
682 terraces and implications for ecosystem services and climate adaptation. *Geomorphology*,
683 379, 107579. <https://doi.org/10.1016/j.geomorph.2020.107579>
- 684 Cammeraat, E. L. H., 2004. Scale dependent thresholds in hydrological and erosion response of a
685 semi-arid catchment in southeast Spain. *Agriculture, Ecosystems and Environment*,
686 104(2), 317–332. <https://doi.org/10.1016/j.agee.2004.01.032>
- 687 Casagli, N., Intrieri, E., Tofani, V., Gigli, G., Raspini, F., 2023. Landslide detection, monitoring
688 and prediction with remote-sensing techniques. *Nature Reviews Earth and Environment*,
689 4(1), 51–64. <https://doi.org/10.1038/s43017-022-00373-x>
- 690 Cevasco, A., Brandolini, P., Scopesi, C., Rellini, I., 2013. Relationships between geo-hydrological
691 processes induced by heavy rainfall and land-use: The case of 25 October 2011 in the
692 Vernazza catchment (Cinque Terre, NW Italy). *Journal of Maps*, 9(2), 289–298.
693 <https://doi.org/10.1080/17445647.2013.780188>
- 694 Chen, C. , Huang, W., 2013. Land use change and landslide characteristics analysis for
695 community-based disaster mitigation. *Environmental Monitoring and Assessment*, 185(5),
696 4125-4139. <https://doi.org/10.1007/s10661-012-2855-y>
- 697 Chen, Y., Vanmaercke, M., Jiao, J., Bai, L., Tang, B., Wang, N., Zhang, Y., Wang, H., 2023.
698 Quantifying the importance of different erosion processes and soil and water conservation
699 measure collapses following an extreme rainstorm in the Chinese Loess Plateau. *Land
700 Degradation and Development*, 34 (2), 403-422. <https://doi.org/10.1002/ldr.4468>
- 701 Clarke, B., Burbank, D., 2010. Bedrock fracturing, threshold hillslopes, and limits to the magnitude
702 of bedrock landslides. *Earth and Planetary Science Letters*, 297, 577-586. <https://doi.org/10.1016/j.epsl.2010.07.011>
- 704 Corominas, J., van Westen, C., Frattini, P., Cascini, L., Malet, J. P., Fotopoulou, S., Catani, F.,
705 Van Den Eeckhaut, M., Mavrouli, O., Agliardi, F., Pitilakis, K., Winter, M. G., Pastor, M.,
706 Ferlisi, S., Tofani, V., Hervás, J., Smith, J. T., 2014. Recommendations for the quantitative
707 analysis of landslide risk. *Bulletin of Engineering Geology and the Environment*, 73(2),
708 209–263. <https://doi.org/10.1007/s10064-013-0538-8>
- 709 Critchley, W., Bruijnzeel, L., 1995. Terrace risers: Erosion control or sediment source. In
710 Sustainable Reconstruction of Highland and Headwater Regions; Singh, R.B.A., Haigh,
711 M.J., Eds.; Oxford and IBH Publishing: New Delhi, India; pp. 529–541
- 712 Crosta, G. B., Dal Negro, P., Frattini, P., 2003. Soil slips and debris flows on terraced slopes.
713 *Natural Hazards and Earth System Science*, 3(1/2), 31–42. <https://doi.org/10.5194/nhess-3-31-2003>
- 714 Crozier, M. J., Glade, T., 2005. Landslide Hazard and Risk: Issues, Concepts and Approach. In
715 Landslide Hazard and Risk. <https://doi.org/10.1002/9780470012659.ch1>
- 717 Das, B.M., 2010. Principles of geotechnical engineering, 7th ed. Cengage Learning. CENGAGE
718 Learning, Stamford.

- 719 de Graaff, J., Amsalu, A., Bodnár, F., Kessler, A., Posthumus, H., Tenge, A., 2008. Factors
 720 influencing adoption and continued use of long-term soil and water conservation measures
 721 in five developing countries. *Applied Geography*, 28(4), 271–280.
 722 <https://doi.org/10.1016/j.apgeog.2008.05.001>
- 723 Deijns, A. A. J., Dewitte, O., Thiery, W., d'Oreye, N., Malet, J.-P., Kervyn, F. 2022. Timing
 724 landslide and flash flood events from SAR satellite: a regionally applicable methodology
 725 illustrated in African cloud-covered tropical environments. *Natural Hazards and Earth
 726 System Sciences*, 22(11), 3679–3700. <https://doi.org/10.5194/nhess-22-3679-2022>
- 727 Deijns, A. A., Michéa, D., Déprez, A., Malet, J.-P., Kervyn, F., Thiery, W., Dewitte, O., 2024. A
 728 semi-supervised multi-temporal landslide and flash flood event detection methodology for
 729 unexplored regions using massive satellite image time series. *ISPRS Journal of
 730 Photogrammetry and Remote Sensing*, 215, 400-418.
 731 <https://doi.org/10.1016/j.isprsjprs.2024.07.010>
- 732 Deng, Chuxiong, Zhang, G., Liu, Y., Nie, X., Li, Z., Liu, J., Zhu, D., 2021. "Advantages and
 733 disadvantages of terracing: A comprehensive review." *International Soil and Water
 734 Conservation Research*, 9(3), 344-359.
- 735 Depicker, A., Govers, G., Jacobs, L., Campforts, B., Uwihirwe, J., Dewitte, O., 2021a. Interactions
 736 between deforestation, landscape rejuvenation, and shallow landslides in the North
 737 Tanganyika-Kivu rift region, Africa. *Earth Surface Dynamics*, 9(3), 445–462.
 738 <https://doi.org/10.5194/esurf-9-445-2021>
- 739 Depicker, A., Jacobs, L., Delvaux, D., Havenith, H.-B., Maki Mateso, J.-C., Govers, G., Dewitte,
 740 O., 2020. The added value of a regional landslide susceptibility assessment: The western
 741 branch of the East African Rift. *Geomorphology*, 353, 106886.
 742 <https://doi.org/10.1016/j.geomorph.2019.106886>
- 743 Depicker, A., Jacobs, L., Mboga, N., Smets, B., Van Rompaey, A., Lennert, M., Wolff, E., Kervyn,
 744 F., Michellier, C., Dewitte, O., Govers, G., 2021b. Historical dynamics of landslide risk
 745 from population and forest-cover changes in the Kivu Rift. *Nature Sustainability*, 4(11),
 746 965–974. <https://doi.org/10.1038/s41893-021-00757-9>
- 747 Dewitte, O., Depicker, A., Moeyersons, J., Dille, A., 2022. Mass Movements in Tropical Climates.
 748 In: Shroder, J.J.F. (Ed.), *Treatise on Geomorphology*, vol. 5. Elsevier, Academic Press, pp.
 749 338–349. <https://doi.org/10.1016/B978-0-12-818234-5.00118-8>, ISBN: 9780128182345
- 750 Dewitte, O., Dille, A., Depicker, A., Kubwimana, D., Maki Mateso, J.-C., Mugaruka Bibentyo, T.,
 751 Uwihirwe, J., Monsieurs, E., 2021. Constraining landslide timing in a data-scarce context:
 752 from recent to very old processes in the tropical environment of the North Tanganyika-
 753 Kivu Rift region. *Landslides*, 18(1), 161–177. <https://doi.org/10.1007/s10346-020-01452-0>
- 754
- 755 Dille, A., Dewitte, O., Handwerger, A. L., d'Oreye, N., Derauw, D., Ganza Bamulezi, G., Ilombe
 756 Mawe, G., Michellier, C., Moeyersons, J., Monsieurs, E., Mugaruka Bibentyo, T.,
 757 Samsonov, S., Smets, B., Kervyn, M., Kervyn, F., 2022. Acceleration of a large deep-
 758 seated tropical landslide due to urbanization feedbacks. *Nature Geoscience*, 15, 1048-1055.
 759 <https://doi.org/10.1038/s41561-022-01073-3>
- 760 Dorren, L., Rey, F., 2004. A review of the effect of terracing on erosion. *Soil Conservation And
 761 Protection for Europe*, 97–108. http://139.191.1.96/projects/scape/transf/Dorren_Rey.pdf
- 762 Dotterweich, M., 2013. The history of human-induced soil erosion: Geomorphic legacies, early
 763 descriptions and research, and the development of soil conservation-A global synopsis.
 764 *Geomorphology*, 201, 1-34. <http://doi.org/10.1016/j.geomorph.2013.07.021>

765 [dataset] Meteo Rwanda, 2022. Historical rainfall data for the northern-western provinces of
766 Rwanda (obtained through the email).

767 Ebabu, K., Tsunekawa, A., Haregeweyn, N., Tsubo, M., Adgo, E., Fenta, A. A., Poesen, J., 2022.
768 Global analysis of cover management and support practice factors that control soil erosion
769 and conservation. *International Soil and Water Conservation Research*, 10(2), 161-176.

770 Fashaho, A., Ndegwa, G. M., Lelei, J. J., Musandu, A. O., Mwonga, S. M., 2020. Effect of land
771 terracing on soil physical properties across slope positions and profile depths in medium
772 and high altitude regions of Rwanda. *South African Journal of Plant and Soil*, 37(2), 91–
773 100. <https://doi.org/10.1080/02571862.2019.1665722>

774 Food and Agriculture Organization (FAO)., 2000. Manual on integrated soil management and
775 conservation practices. *FAO Land and Water Bulletin*, 8(ISBN 92-5-104417-1), 15–214.

776 Gabet, E., Dunne, T., 2002. Landslides on coastal sage-scrub and grassland hillslopes in a severe
777 El Niño winter: The effects of vegetation conversion on sediment delivery. *Bulletin of the*
778 *Geological Society of America*, 114 (8), 983-990. [https://doi.org/10.1130/0016-
779 7606\(2002\)114<0983:LOCSSA>2.0.CO;2](https://doi.org/10.1130/0016-7606(2002)114<0983:LOCSSA>2.0.CO;2)

780 Garden, R. A. M., Gerard, A. J., 2003. Runoff and soil erosion on cultivated rainfed terraces in the
781 Middle Hills of Nepal

782 García-Ruiz, J. M., Nadal-Romero, E., Lana-Renault, N., Beguería, S., 2013. Erosion in
783 Mediterranean landscapes: Changes and future challenges. *Geomorphology*, 198, 20–36.
784 <https://doi.org/10.1016/j.geomorph.2013.05.023>

785 Gariano, S. L., Guzzetti, F., 2016. Landslides in a changing climate. *Earth-Science Reviews*, 162,
786 227-252. <http://dx.doi.org/10.1016/j.earscirev.2016.08.011>

787 Glade, T., 2003. Landslide occurrence as a response to land use change: A review of evidence
788 from New Zealand. *Catena*, 51, 297-314. [https://doi.org/10.1016/S0341-8162\(02\)00170-
789 7](https://doi.org/10.1016/S0341-8162(02)00170-7)

789 Glade, T., Anderson, M., Crozier, M. J., 2012. *Landslide Hazard and Risk*. John Wiley & Sons
790 Ltd.; 111 River Street, Hoboken, NJ 07030, USA <https://doi.org/10.1002/9780470012659>

791 Guzzetti, F., Mondini, Alessandro C., Cardinali, M., Fiorucci, F., Santangelo, M., Chang, K. T.,
792 2012. Landslide inventory maps: New tools for an old problem. *Earth-Science Reviews*,
793 112, 42-66. <http://dx.doi.org/10.1016/j.earscirev.2012.02.001>

794 Guzzetti, F., Peruccacci, S., Rossi, M., Stark, C. P., 2007. Rainfall thresholds for the initiation of
795 landslides in central and southern Europe. *Meteorology and Atmospheric Physics*, 267,
796 239–267. <https://doi.org/10.1007/s00703-007-0262-7>

797 Hungr, O., Leroueil, S., Picarelli, L., 2014. The Varnes classification of landslide types, an update.
798 *Landslides*, 11(2), 167-194. <https://doi.org/10.1007/s10346-013-0436-y>

799 Japan Aerospace Exploration Agency (JAXA), 2011. Radiometric terrain correction. Accessed
800 through:<https://asf.alaska.edu/datasets/daac/alos-palsar-radiometric-terrain-correction/>

801 Jacobs, L., Dewitte, O., Poesen, J., Delvaux, D., Thiery, W., Kervyn, M., 2016. The Rwenzori
802 Mountains, a landslide-prone region? *Landslides* 13, 519–536. doi:10.1007/s10346-015-
803 0582-5

804 Jones, J.N., Boulton, S.J., Bennett, G.L., Stokes, M., Bennett, G.L., Whitworth, M.R.Z., 2021. 30-
805 year record of Himalaya mass-wasting reveals landscape perturbations by extreme events.
806 *Nature Communications* 12, 6701. doi:10.1038/s41467-021-26964-8

807 Kagabo, D. M., Stroosnijder, L., Visser, S. M., & Moore, D., 2013. Soil erosion, soil fertility and
808 crop yield on slow-forming terraces in the highlands of Buberuka, Rwanda. *Soil and*
809 *Tillage Research* , 128, 23-29. <http://dx.doi.org/10.1016/j.still.2012.11.002>

810 Kitutu, M. G., Muwanga, A., Poesen, J., Deckers, J. A., 2011. Farmer's perception on landslide
811 occurrences in Bududa District, Eastern Uganda. *African Journal of Agricultural Research*,
812 6(1); 7-18. <https://doi.org/10.5897/AJAR09.158>

813 Koulouri, M., Giourga, C., 2007. Land abandonment and slope gradient as key factors of soil
814 erosion in Mediterranean terraced lands. *Catena*, 69(3), 274–281.
815 <https://doi.org/10.1016/j.catena.2006.07.001>

816 Kuria, A. W., Barrios, E., Pagella, T., Muthuri, C. W., Mukuralinda, A., Sinclair, F. L., 2019.
817 Farmers' knowledge of soil quality indicators along a land degradation gradient in Rwanda.
818 *Geoderma Regional*, 16, e00199. <https://doi.org/10.1016/j.geodrs.2018.e00199>

819 LaFevor, M. C., 2014. Restoration of degraded agricultural terraces: Rebuilding landscape
820 structure and process. *Journal of Environmental Management*, 138, 32–42.
821 <https://doi.org/10.1016/j.jenvman.2013.11.019>

822 Lee, S., Pradhan, B., 2007. Landslide hazard mapping at Selangor, Malaysia using frequency ratio
823 and logistic regression models. *Landslides*, 4(1), 33-41. [https://doi.org/10.1007/s10346-](https://doi.org/10.1007/s10346-006-0047-y)
824 [006-0047-y](https://doi.org/10.1007/s10346-006-0047-y)

825 Lesschen, J. P., L. H., Cammeraat, T. N., 2008. Erosion and terrace failure due to agricultural land
826 abandonment in a semi-arid environment. *Earth Surf. Process. Landforms*, 33(1676),
827 1574–1584. <https://doi.org/DOI:10.1002/esp.1676>

828 Lewis, L. A., 1992. Terracing and accelerated soil loss on rwandian steep lands: A preliminary
829 investigation of the implications of human activities affecting soil movement. *Land*
830 *Degradation & Development*, 3(4), 241–246. <https://doi.org/10.1002/ldr.3400030405>

831 Lewis, L. A., Nyamulinda, V., 1996. The critical role of human activities in land degradation in
832 Rwanda. *Land Degradation & Development*, 7(1), 47–55.
833 [https://doi.org/10.1002/\(sici\)1099-145x\(199603\)7:1<47::aid-ldr213>3.3.co;2-d](https://doi.org/10.1002/(sici)1099-145x(199603)7:1<47::aid-ldr213>3.3.co;2-d)

834 Lewis, S. L., Edwards, D. P., Galbraith, D., 2015. Increasing human dominance of tropical forests.
835 *Science*, 349(6250), 827–832.

836 Londoño, Ana C., 2008. Pattern and rate of erosion inferred from Inca agricultural terraces in arid
837 southern Peru. *Geomorphology*, 99, 13-25. [https://doi.org/](https://doi.org/10.1016/j.geomorph.2007.09.014)
838 [10.1016/j.geomorph.2007.09.014](https://doi.org/10.1016/j.geomorph.2007.09.014)

839 Londoño, A. C., Williams, P. R., Hart, M. L., 2017. A change in landscape: Lessons learned from
840 abandonment of ancient Wari agricultural terraces in Southern Peru. *Journal of*
841 *Environmental Management*, 202, 532–542.
842 <https://doi.org/10.1016/j.jenvman.2017.01.012>

843 Maes, J., Kervyn, M., de Hontheim, A., Dewitte, O., Jacobs, L., Mertens, K., Vanmaercke, M.,
844 Vranken, L., Poesen, J., 2017. Landslide risk reduction measures: A review of practices
845 and challenges for the tropics. *Progress in Physical Geography*, 41(2), 191-221.
846 <https://doi.org/10.1177/0309133316689344>

847 Maki Mateso, J. -C., Biolders, C. L., Monsieurs, E., Depicker, A., Smets, B., Tambala, T., Bagalwa
848 Mateso, L., Dewitte, O., 2023. Characteristics and causes of natural and human-induced
849 landslides in a tropical mountainous region: the rift flank west of Lake Kivu (Democratic
850 Republic of the Congo). *Natural Hazards and Earth System Sciences*, 23(2), 643–666.
851 <https://doi.org/10.5194/nhess-23-643-2023>

852 Malamud, B. D., Turcotte, D. L., Guzzetti, F., Reichenbach, P., 2004. Landslide inventories and
853 their statistical properties. *Earth Surface Processes and Landforms*, 29 (6), 687-711.
854 <https://doi.org/10.1002/esp.1064>

855 Mesfin, A., 2016. A Field Guideline on Bench Terrace Design and Construction. Ministry of
856 Agriculture and Natural Resources Natural Resource Management Directorate, October,
857 44.

858 Milledge, D. G., Bellugi, D., McKean, J. A., Densmore, A. L., Dietrich, W. E., 2014. A
859 multidimensional stability model for predicting shallow landslide size and shape across
860 landscapes. *Journal of Geophysical Research: Earth Surface*, 119(11), 2481–2504.
861 <https://doi.org/10.1002/2014JF003135>

862 MINEMA., 2018. National contingency plan for floods and landslides. 23.
863 <https://www.minema.gov.rw/publications>

864 Ministry of Environment., 2018. Upper Nyabarongo catchment management plan 2018-
865 2024.[Technical report published by Rwanda Ministry of Environment].
866 <https://waterportal.rwb.rw/node/3136>

867 Monsieus, E., Kirschbaum, D., Thiery, W., van Lipzig, N., Kervyn, M., Demoulin, A., Jacobs, L.,
868 Kervyn, F., Dewitte, O., 2017. Constraints on Landslide-Climate Research Imposed by the
869 Reality of Fieldwork in Central Africa. In: De Graff, J. V., Shakoor, A. (eds.), 3rd North
870 American Symposium on Landslides: Landslides: Putting Experience, Knowledge, and
871 Emerging Technologies into Practice. Association of Environmental & Engineering
872 Geologists (AEG), pp. 158–168. ISBN 978-0-9897253-7-8.

873 Monsieus, E., Jacobs, L., Michellier, C., Basimike Tchangaboba, J., Bamulezi Ganza, G., Kervyn,
874 F., Maki Mateso, J.-C., Mugaruka Bibentyo, T., Kalikone Buzera, C., Nahimana, L.,
875 Ndayisenga, A., Nkurunziza, P., Thiery, W., Demoulin, A., Kervyn, M., Dewitte, O.,
876 2018a. Landslide inventory for hazard assessment in a data-poor context: a regional-scale
877 approach in a tropical African environment. *Landslides* 15, 2195–2209.
878 doi:10.1007/s10346-018-1008-y

879 Monsieus, E., Kirschbaum, D.B., Tan, J., Maki Mateso, J.-C., Jacobs, L., Plisnier, P.-D., Thiery,
880 W., Augusta, U., Didace, M., Mugaruka Bibentyo, T., Bamulezi Ganza, G., Ilombe Mawe,
881 G., G., Bagalwa, L., Kankurize, C., Michellier, C., Stanley, T., Kervyn, F., Kervyn, M.,
882 Demoulin, A., Dewitte, O., 2018b. Evaluating TMPA rainfall over the sparsely gauged
883 East African Rift. *Journal of Hydrometeorology*, 19(9): 1507-1528.
884 <https://doi.org/10.1175/JHM-D-18-0103.1>

885 Monsieus, E., Dewitte, O., Demoulin, A., 2019. A susceptibility-based rainfall threshold approach
886 for landslide occurrence. *Natural Hazards and Earth System Sciences* 19, 775–789.
887 doi:10.5194/nhess-19-775-2019

888 Mugaruka Bibentyo T., Dille, A., Depicker, A., Smets, B., Vanmaercke, M., Nzolanga, C.,
889 Dewaele, S., Dewitte, O., 2024. Landslides, bedrock incision and human-induced
890 environmental changes in an extremely rapidly formed tropical river gorge.
891 *Geomorphology*, 109046, 7823–7830. <https://doi.org/10.1016/j.geomorph.2023.109046>

892 Nambajimana, J., He, X., Zhou, J., Justine, M. F., Li, J., Khurram, D., Mind'je, R., Nsabimana, G.,
893 2020. Land use change impacts on water erosion in Rwanda. *Sustainability*, 12(1), 1-23.
894 <https://doi.org/10.3390/SU12010050>

895 Nakulopa, F., Vanderkelen, I., Van de Walle, J., van Lipzig, N.P.M., Tabari, H., Jacobs, L.,
896 Tweheyo, C., Dewitte, O., Thiery, W., 2022. Evaluation of High-Resolution Precipitation
897 Products over the Rwenzori Mountains (Uganda). *Journal of Hydrometeorology* 23, 747–
898 768. doi:10.1175/jhm-d-21-0106.1

899 Niyokwiringirwa, P., Lombardo, L., Dewitte, O., Deijns, A.A.J., Wang, N., van Westen, C.,
900 Tanyas, H., 2024. Event-based rainfall-induced landslide inventories and rainfall

901 thresholds for Malawi. *Landslides* 21, 1403-1424. [https://doi.org/10.1007/s10346-023-](https://doi.org/10.1007/s10346-023-02203-7)
902 02203-7.

903 Niyonzima, O., 2018. Grief and horror as landslide victims are buried in western Rwanda.
904 Retrieved from [https://www.ktpress.rw/2018/05/grief-and-horror-as-landslide-victims-](https://www.ktpress.rw/2018/05/grief-and-horror-as-landslide-victims-are-buried-in-western-rwanda/)
905 [are-buried-in-western-rwanda/](https://www.ktpress.rw/2018/05/grief-and-horror-as-landslide-victims-are-buried-in-western-rwanda/)

906 Ozturk, U., Bozzolan, E., Holcombe, E. A., Shukla, R., Pianosi, F., Wagener, T., 2022. How
907 climate change and unplanned urban sprawl bring more landslides. *Nature*, 608(7922),
908 262–265. <https://doi.org/10.1038/d41586-022-02141-9>

909 Pedregosa, F., Varoquaux, G., Gramfort, A., Michel, V., Thirion, B., Grisel, O., Duchesnay, É.,
910 2011. Scikit-learn: Machine learning in Python. *the Journal of Machine Learning Research*,
911 12, 2825-2830.

912 Pepe, G., Mandarino, A., Raso, E., Scarpellini, P., Brandolini, P., Cevasco, A., 2019. Investigation
913 on farmland abandonment of terraced slopes using multitemporal data sources comparison
914 and its implication on hydro-geomorphological processes. *Water*, 11.
915 <https://doi.org/10.3390/w11081552>

916 Petley, D. N., Hearn, G. J., Hart, A., Rosser, N. J., Dunning, S. A., Owen, K., Mitchell, W. A.,
917 2007. Trends in landslide occurrence in Nepal. *Natural Hazards*, 43 (1), 23-44.
918 <https://doi.org/10.1007/s11069-006-9100-3>

919 Pijl, A., Quarella, E., Vogel, T. A., D'Agostino, V., Tarolli, P., 2021. Remote sensing vs. field-
920 based monitoring of agricultural terrace degradation. *International Soil and Water*
921 *Conservation Research*, 9(1), 1–10. <https://doi.org/10.1016/j.iswcr.2020.09.001>

922 Posthumus, H., 2005. Adoption of terraces in the Peruvian Andes. In *Tropical Resource*
923 *Management Papers* (Vol. 72).

924 Regional Centre Mapping Resources and Development (RCMRD)., 2015. Map of land use of
925 Rwanda. Retrieved from
926 https://geoportal.rcmrd.org/layers/servir%3A Rwanda_landcover_2015_scheme_ii

927 Reichenbach, P., Rossi, M., Malamud, B. D., Mihir, M., Guzzetti, F., 2018. A review of
928 statistically-based landslide susceptibility models. *Earth-Science Reviews*, 180, 60–91.
929 <https://doi.org/10.1016/j.earscirev.2018.03.001>

930 Rickli, C., Graf, F., 2009. Effects of forests on shallow landslides - Case studies in Switzerland.
931 *Forest Snow and Landscape Research*, 82 (1), 33-44.

932 Romero Díaz, A., Marín Sanleandro, P., Sánchez Soriano, A., Belmonte Serrato, F., Faulkner, H.,
933 2007. The causes of piping in a set of abandoned agricultural terraces in southeast Spain.
934 *Catena*, 69(3), 282–293. <https://doi.org/10.1016/j.catena.2006.07.008>

935 Roose, E., Ndayizigiye, F., 1997. Agroforestry, water and soil fertility management to fight erosion
936 in tropical mountains of Rwanda. *Soil Technology*, 11(1), 109–119.
937 [https://doi.org/10.1016/S0933-3630\(96\)00119-5](https://doi.org/10.1016/S0933-3630(96)00119-5)

938 Rossi, M., Guzzetti, F., Reichenbach, P., Mondini, A.C., Peruccacci, S., 2010. Optimal landslide
939 susceptibility zonation based on multiple forecasts. *Geomorphology* 114, 129–142,
940 <http://dx.doi.org/10.1016/j.geomorph.2009.06.020>

941 Rutebuka, J., Munyeshuli, A. U., Nkundwakazi, O., Mbarushimana, D. K., Mbonigaba, J. J. M.,
942 Vermeir, P., Verdoodt, A., 2021. Effectiveness of terracing techniques for controlling soil
943 erosion by water in Rwanda. *Journal of Environmental Management*, 277, 111369.
944 <https://doi.org/10.1016/j.jenvman.2020.111369>

945 Sasahara, K., Sakai, N., 2014. Development of shear deformation due to the increase of pore
946 pressure in a sandy model slope during rainfall. *Engineering Geology*, 170, 43-51.

947 Sekajugo, J., Kagoro-Rugunda, G., Mutyeber, R., Kabaseke, C., Namara, E., Dewitte, O., Kervyn,
948 M., Jacobs, L., 2022. Can citizen scientists provide a reliable geo-hydrological hazard
949 inventory? An analysis of biases, sensitivity and precision for the Rwenzori Mountains,
950 Uganda. *Environmental Research Letters* 17, 045011. doi:10.1088/1748-9326/ac5bb5

951 Schilirò, L., Cevasco, A., Esposito, C., Mugnozza, G. S., 2018. Shallow landslide initiation on
952 terraced slopes: inferences from a physically based approach. *Geomatics, Natural Hazards
953 and Risk*, 9(1), 295-324.

954 Schuster, R. L., Highland, L. M., 2001. Socioeconomic and environmental impacts of landslides
955 in the Western Hemisphere. U.S. Geological Survey, pp47

956 Seto, K. C., Güneralp, B., Hutyra, L. R., 2012. Global forecasts of urban expansion to 2030 and
957 direct impacts on biodiversity and carbon pools. *Proceedings of the National Academy of
958 Sciences of the United States of America*, 109(40), 16083–16088.
959 <https://doi.org/10.1073/pnas.1211658109>

960 Sidle, R. C., Bogaard, T. A., 2016. Dynamic earth system and ecological controls of rainfall-
961 initiated landslides. *Earth-Science Reviews*, 159, 275-291.

962 Sidle, R. C., Ziegler, A. D., Negishi, J. N., Nik, A. R., Siew, R., Turkelboom, F., 2006. Erosion
963 processes in steep terrain - Truths, myths, and uncertainties related to forest management
964 in Southeast Asia. *Forest Ecology and Management*, 224(1–2), 199–225.
965 <https://doi.org/10.1016/j.foreco.2005.12.019>

966 Stoltzfus, J. C., 2011. Logistic regression: A brief primer. *Academic Emergency Medicine*, 18(10),
967 1099–1104. <https://doi.org/10.1111/j.1553-2712.2011.01185.x>

968 Tanyaş, H., Allstadt, K. E., van Westen, C. J., 2018. An updated method for estimating landslide-
969 event magnitude. *Earth surface processes and landforms*, 43(9), 1836-1847.

970 Tarolli P., Preti, F., Romano, N., 2014. Terraced landscapes: From an old best practice to a
971 potential hazard for soil degradation due to land abandonment. *Anthropocene*, 6,10-25.
972 <http://dx.doi.org/10.1016/j.ancene.2014.03.002>

973 Terajima, T., Miyahira, E. I., Miyajima, H., Ochiai, H., Hattori, K., 2014. How hydrological factors
974 initiate instability in a model sandy slope. *Hydrological Processes*, 28(23), 5711-5724.

975 Theunissen, K., Hanon, M., Fernandez, M., 1991. Carte Géologique du Rwanda-Scale: 1/250000.
976 Royal Museum for Central Africa, Tervuren, Belgium.

977 Thomas, M.A., Collins, B.D., Mirus, B.B., 2019. Assessing the Feasibility of Satellite-Based
978 Thresholds for Hydrologically Driven Landsliding, *Water Resources Research*.
979 <https://doi.org/10.1029/2019WR025577>

980 Thomas, M.A., Mirus, B.B., Smith, J.B., 2020. Hillslopes in humid-tropical climates aren't always
981 wet: Implications for hydrologic response and landslide initiation in Puerto Rico.
982 *Hydrological Processes*, 34, 4307-4318. <https://doi.org/10.1002/hyp.13885>

983 Turkelboom, F., Poesen, J., Trébuil, G., 2008. The multiple land degradation effects caused by
984 land-use intensification in tropical steeplands: A catchment study from northern Thailand.
985 *Catena*, 75, 102–116. <https://doi.org/10.1016/j.catena.2008.04.012>

986 Uwacu, R. A., Habanabakize, E., Adamowski, J., Schwinghamer, T. D., 2021. Using radical
987 terraces for erosion control and water quality improvement in Rwanda: A case study in
988 Sebeya catchment. *Environmental Development*, 39, 100649.
989 <https://doi.org/10.1016/j.envdev.2021.100649>

990 Uwihirwe, J., Hrachowitz, M., Bogaard, T.A., 2020. Landslide precipitation thresholds in Rwanda.
991 *Landslides* 17, 2469–2481. doi:10.1007/s10346-020-01457-9

992 Uwihirwe, J., Hrachowitz, M., Bogaard, T., 2022. Integration of observed and model-derived
 993 groundwater levels in landslide threshold models in Rwanda. *Natural Hazards and Earth*
 994 *System Sciences*, 22(5), 1723-1742.
 995 Van Den Eeckhaut, M., Poesen, J., Govers, G., Verstraeten, G., Demoulin, A., 2007.
 996 Characteristics of the size distribution of recent and historical landslides in a populated
 997 hilly region. *Earth and Planetary Science Letters*, 256(3-4), 588-603.
 998 Van Dijk, A.I.J.M., Bruijnzeel, L. A., 2004. Runoff and soil loss from bench terraces.2. An event-
 999 based erosion process model. *European Journal of Soil Science*, 55, 317-334.
 1000 [https://doi.org/ 10.1111/j.1365-2389.2004.00605.x](https://doi.org/10.1111/j.1365-2389.2004.00605.x)
 1001 Water for Growth Rwanda., 2018. Integrated Water Resources Management Program Rwanda:
 1002 Sebeya catchment plan 2018-2024 [Technical report published by the Rwanda Ministry of
 1003 Environment].[https://waterportal.rwb.rw/sites/default/files/201904/Sebeya%20Catchment](https://waterportal.rwb.rw/sites/default/files/201904/Sebeya%20Catchment%20Plan_0.pdf)
 1004 [%20Plan_0.pdf](https://waterportal.rwb.rw/sites/default/files/201904/Sebeya%20Catchment%20Plan_0.pdf)
 1005 Wei, W., Chen, D., Wang, L., Daryanto, S., Chen, L., Yu, Y., Lu, Y., Sun, G., Feng, T., 2016.
 1006 Global synthesis of the classifications, distributions, benefits and issues of terracing. *Earth-*
 1007 *Science Reviews*, 159(18), 388–403. <https://doi.org/10.1016/j.earscirev.2016.06.010>
 1008 Wicki, A., Jansson, P.E., Lehmann, P., Hauck, C., Stähli, M., 2021. Simulated or measured soil
 1009 moisture: Which one is adding more value to regional landslide early warning? *Hydrol.*
 1010 *Earth Syst. Sci.* 25, 4585–4610. <https://doi.org/10.5194/hess-25-4585-2021>
 1011 Williams, L. S., 1990. Agricultural terrace evolution in Latin America. *Yearbook - Conference of*
 1012 *Latin Americanist Geographers*, 16, 82–93.
 1013 Wolter, A., Ward, B., Millard, T., 2010. Instability in eight sub-basins of the Chilliwack River
 1014 Valley, British Columbia, Canada: A comparison of natural and logging-related landslides.
 1015 *Geomorphology*, 120, 123-132. <http://dx.doi.org/10.1016/j.geomorph.2010.03.008>
 1016 Zhou, C. H., Lee, C.F., Li, J., Xu, Z. W., 2002. On the spatial relationship between landslides and
 1017 causative factors on Lantau Island, Hong Kong. *Geomorphology*, 43, 197-207.
 1018 [https://doi.org/ 10.1016/S0169-555X\(01\)00130-1](https://doi.org/10.1016/S0169-555X(01)00130-1)